Classification: Biological Sciences, Evolution

Title: Olfactory receptors tuned to volatile mustard oils in drosophilid flies

Authors: *Teruyuki Matsunaga[1], *Carolina E. Reisenman[2], *Benjamin Goldman-Huertas[3], Philipp Brand[4], Kevin Miao[1], Hiromu Suzuki[1], Santiago R. Ramírez[4], Noah K. Whiteman[1#]

*Equal contributions

Affiliations:

1 Department of Integrative Biology, University of California Berkeley, Berkeley, CA

2 Department of Molecular and Cell Biology, University of California Berkeley, Berkeley, CA

3 Department of Molecular and Cellular Biology, University of Arizona, Tucson, AZ

4 Department of Evolution and Ecology, University of California Davis, Davis, CA

[#]Correspondence to: whiteman@berkeley.edu (N.K.W.)

Keywords:

Scaptomyza flava, *Drosophila melanogaster*, herbivory, evolution, olfaction, isothiocyanate, chemoreceptor, olfactory receptor, TrpA1, wasabi, Or67b

Abstract (248):

Plant toxins are effective defenses because they are aversive to most insects. The same molecules, however, are co-opted as host-finding cues by specialist herbivores. Although these behavioral shifts are central to our understanding of herbivorous insect diversification, it is not well understood how these behaviors evolve. We addressed this in *Scaptomyza flava,* a herbivorous drosophilid fly that shifted to toxic mustard plants (Brassicales) less than 10 million years ago and lost the ancestral attraction to yeast volatiles as well as the attendant chemoreceptors. We first found a gain-of-function behavior: *S. flava*, but not its close microbe-feeding relatives *Drosophila melanogaster* and *S. pallida*, is attracted to mustard host-plant odors, including volatile mustard oils (isothiocyanates or ITCs). Our genomic analysis then uncovered three *S. flava* paralogs of an olfactory receptor gene (*Or67b*) that likely experienced recent positive selection. We then tested whether these candidate chemoreceptors could underlie the observed attraction to volatile ITCs. Our *in vivo* recordings revealed that two of the *S. flava* Or67b proteins (Or67b1 and Or67b3) – but not the homologous Ors from microbe-feeding relatives - responded selectively to volatile ITCs. These Ors are the first ITC chemoreceptors other than TRP channel family (*e.g.*, the TrpA1 'wasabi' receptor) known from any animal. Remarkably, *S. flava Or67b3* was sufficient to drive olfactory attraction toward butyl ITC when expressed in an attractive olfactory circuit. Our study illuminates that ancestrally aversive chemicals can be co-opted as attractants through gene duplication, leading to the origin of hedonic valence shifts in herbivorous insects.

Significance Statement (120)

Plant toxins trigger aversive olfactory (volatile-mediated) and gustatory (contact-mediated) responses in most animals. Paradoxically, toxic plants are often colonized by specialist insects that co-opt these toxins for host-plant finding. The mechanisms underlying these behavioral shifts, from indifference or repulsion to attraction, remain unclear. To address this gap in our knowledge, we used a fly lineage, *Scaptomyza*, that switched from yeast-feeding to feeding on mustard plants less than 10 million years ago. We found that *Scaptomyza* is attracted to mustard-plant odors and volatile mustard oils (isothiocyanates or ITCS) such as 'wasabi', a behavior enabled by the evolution of genes encoding odorant receptors highly sensitive and selective to ITCs. Our study illuminates how insects colonize toxic host plants by through duplication and ecological repurposing of genes encoding pre-existing chemoreceptors.

INTRODUCTION

Many plant compounds used in food, agriculture and medicine originally evolved as toxins that deter and repel enemies (1). Among the most well-known compounds are those reactive electrophiles that induce the sensation of pain, such as diallyl disulfide and thiosulfinates produced by Alliaceae plants (*e.g.*, onions and relatives), α,β-unsaturated aldehydes found in Lauraceae (*e.g.*, cinnamon and olives), and isothiocyanates (ITCs) from mustards and their relatives in the Brassicales. Paradoxically, herbivores that specialize on these plants have evolved electrophile diversion or resistance mechanisms and use these plants as a food source and habitat (2, 3). Interestingly, mustard specialists can be trapped with ITC baits, indicating that specialists use "aversive" electrophiles for host finding (4). However, the mechanisms mediating the detection of species-specific electrophiles, as well as the mechanisms underlying shifts in hedonic valence, are relatively unknown.

In animals, the only known and broadly conserved electrophile detecting sensors are the Transient Receptor Potential (TRP) nociceptive channel family (5–7), and the most studied among them is the Transient Receptor Potential Ankyrin-1 (TrpA1) (8-10). Reactive electrophiles form covalent adducts with cysteine and lysine residues in TrpA1, activating this non-selective cation channel and resulting in the perception of pain (9). A reasonable hypothesis explaining the attraction of specialist mustard-plant insects to host-plant-derived electrophiles is that the *TrpA1* circuit has shifted from an aversive to an attractive one. However, TrpA1 is a gustatory, non-selective electrophile sensor activated by myriad electrophiles produced by plants in different orders, including diallyl disulfide, cinnamaldehyde, and ITCs, rendering this chemoreceptor ineffective in signaling host-plant identity (7). Alternatively, chemoreceptor proteins (*e.g.*, olfactory receptors -Ors- and/or ionotropic receptors -Irs-) that commonly mediate

responses to volatile compounds in insects (11, 12) are better suited to evoke responses that signal volatile, host-specific electrophiles. Specificity for ecologically relevant volatiles repeatedly arose through evolution of these olfactory chemoreceptors (13, 14). In *D. sechellia*, a specialist of the toxic "noni fruit", Ir75b evolved high sensitivity to a signature noni volatile through a single amino acid residue substitution (15). Similarly, in other drosophilid species, Or22a (and Or22b) evolved to be narrowly tuned to host-plant volatile esters (16, 17), facilitating host-plant specialization.

Here, we investigate the evolutionary and functional mechanisms underlying a major shift in host plant use: olfactory specialization on mustard plants by *S. flava*. *S. flava* is a relative of *D. melanogaster* nested phylogenetically in the paraphyletic *Drosophila* subgenus and a specialist herbivore of ITCs-producing Brassicales plants (18, 19). In behavioral olfactory assays, we found that *S. flava*, but not its microbe-feeding relatives *S. pallida* or *D. melanogaster*, is attracted to volatile ITCs and odors from Brassicales plants. We scanned the genome sequence of *S. flava* to identify rapidly evolving chemoreceptors as candidates underlying this behavioral shift, and identified a lineage-specific expansion of three paralogous copies of the olfactory receptor gene *Or67b* that exhibited signatures of positive selection in the *S. flava* lineage. This *Or*, in contrast, is present as a single copy and is under strong evolutionary constraint in *S. pallida* and *D. melanogaster*. *In vivo* functional testing of Or67b copies from these species shows that two *S. flava* Or67b receptors, but not the conserved Or67b variants from its microbe-feeding relatives, responded sensitively and selectively to volatile ITCs. Furthermore, *D. melanogaster* flies expressing *S. flava Or67b3* were attracted to butyl ITC in olfactory assays, indicating that this receptor may be sufficient for attraction to volatile ITCs in this context. We also found that ITCs are not detected through covalent modification of Or67bs, as opposed to TrpA1 (*e.g.* (7)).

Or67b *S. flava* proteins selectively shifted their odor-receptive range to ITCs, an entirely new chemical class, from an ancestral olfactome of ketones, alcohols, and aldehydes. In summary, we discovered an evolutionary mechanism by which specialist herbivorous insects can shift hedonic valence from aversion to attraction towards host plant-specific electrophiles. A novel ITC-sensitive olfactory receptor system supplements the generalist TRP sensory system of a mustard specialist, an adaptation that evolved through gene duplication and neofunctionalization.

RESULTS

S. flava is attracted to mustard plant odors and volatile ITCs

Because *S. flava* is a Brassicales specialist, we first determined whether this species is attracted to mustard plant volatiles using a dual-choice olfactory assay (based on (20). We found that both adult male and female *S. flava* are attracted to arugula *(Eruca vesicaria)* leaf odors (two-tailed Binomial tests corrected for multiple testing using FDR, $p<0.05$; Fig. 1). In contrast, *D. melanogaster* was neither attracted nor deterred by arugula odors but instead was strongly attracted to apple cider vinegar volatiles ($p=0.0001$, Fig. 1), in agreement with previous results (*e.g.* (21)). In tests with apple cider vinegar, male *S. flava* preferred the odorless arm of the maze ($p<0.05$) and females showed a similar tendency towards apple cider vinegar (FDR adjusted $p=0.0541$). *S. pallida* exhibited an intermediate behavior, distributing equally between the vinegar-laden and the odorless arms of the maze. Overall, these results demonstrate that *S. flava*, but not *D. melanogaster* or *S. pallida*, is attracted to mustard plant volatiles, and avoids odor sources that strongly attract *D. melanogaster*, characterized by the presence of acetic acid and a variety of ester, carbonyl, and hydroxyl-containing compounds (22, 23).

Brassicales plants typically produce ITCs upon tissue damage, which are highly toxic to non-adapted insects but not to mustard specialists, including *S. flava* (24). Moreover, volatile ITCs are effective in capturing a variety of distantly related specialist insects in traps (4). We therefore investigated whether the sole presence of ITCs can mediate olfactory attraction in *S. flava*. Adult female *S. flava* were attracted to both butyl ITC and sec-butyl ITC (Fig. 1). Males, in contrast, were only attracted to butyl ITC (Fig. 1), which suggests that at least some ITCs might be involved in mediating sex-specific behaviors. Interestingly, *S. pallida* oriented against butyl ITC (FDR adjusted p-value<0.05), which may be a strategy to avoid ITCs as this species sometimes feed on decomposing -but not intact- mustard leaves. In contrast, *D. melanogaster* flies distributed at random between the arms of the maze regardless of the ITC compound tested (p>0.5), indicating that ITCs do not elicit olfactory attraction in this species. In sum, these experiments demonstrate that *S. flava*, but not its microbe-feeding relatives, is attracted to mustard plant volatiles and ITCs.

Phylogenetic analysis identified *Or67b* paralogs as candidates mediating the detection of ecologically relevant odorants

To identify potential *S. flava* chemosensory receptors involved in the attraction of mustard volatiles, we conducted a phylogenetic analysis of the Or protein sequences of *S. flava* and four other *Drosophila* species to identify *Scaptomyza*-specific losses and gains (Fig. 2*A*). The Or topology was largely congruent with previous *Drosophila* Or trees (25) except for some deeper nodes, which had weak to moderate bootstrap support. In order to identify *Ors* evolving under positive selection in *S. flava*, we inferred d*N*/d*S*, the ratio of nonsynonymous to synonymous substitution rates, using a foreground/background branch test as implemented in

PAML (26). Of 75 *S. flava* branches tested, seven branch models (for paralogs of *Or63a, Or67b* and *Or98a*, and a homolog of *Or67d*) indicated an *S. flava* foreground rate >1, consistent with positive selection (Table S1). Of these receptors, homologs of *Or67d* detect the *Drosophila* pheromone 11-cis-vaccenyl acetate (27) and likely function in intraspecific communication in *Scaptomyza*, *Or63a* is only expressed in larvae (28), and the *Or98a*-like genes found in *Scaptomyza* have no *D. melanogaster* homologs and are functionally uncharacterized. In contrast, *Or67b* is expressed in adults and modulates oviposition behavior (29), suggesting that it is a good candidate for further study. In a previous study, branch-site tests were also consistent with episodic positive selection acting on *Or67b* paralogs from *S. flava* (19). After expanding the representation of *Or67b* homologs in a phylogenetic analysis, and conducting branch tests in PAML on all branches in the tree, we found support for elevated d*N*/d*S* exclusively in *S. flava* and *D. mojavensis* branches (Fig. 2*B*; TableS1). Thus, we focused on *Or67b* paralogs for functional studies.

S. flava Or67b proteins respond specifically to mustard plant volatiles

We investigated whether any of the three *S. flava* Or67b proteins could mediate the odor-specific attraction of *S. flava* to mustard plant volatiles. First, we confirmed that all three paralogs are expressed in adult *S. flava* (Fig. S2*B*). To study the odor-response profile of Or67b across species, we used a *D. melanogaster* mutant that lacks its endogenous olfactory receptor (Or22a) in the ab3A olfactory receptor neuron (known as the "empty neuron system" (30, 31). We conducted single sensillum recordings from the ab3 sensilla in transgenic *D. melanogaster* flies expressing each of the *S. flava* (*Sfla*) *Or67b* paralogs, as well as the *Or67b* orthologs from *S. pallida* (*Spal*) and *D. melanogaster* (*Dmel*) (Fig. 3*A*). *Or22a* deletion in ab3A was confirmed

by the lack of responses in ab3A to ethyl hexanoate, a strong Or22a activator (Fig. S4*A*). We found that ab3A neurons expressing any of the three *Sfla Or67b* paralogs responded to all mustard plant volatiles tested (Fig. 3*B*; Mann-Whitney U tests adjusted for multiple comparisons using FDR, $p<0.05$ in all cases). In contrast, neurons expressing *Dmel Or67b* responded strongly to apple cider vinegar (Mann-Whitney U tests adjusted for multiple comparisons, $p<0.05$), but not to any of the mustard plant volatiles tested ($p>0.1$, Fig. 3*B*). Neurons expressing *Spal Or67b* also showed strong responses when stimulated with apple cider vinegar, but displayed only modest responses to arugula volatiles (Fig. 3*B*). Interestingly, stimulation with apple cider vinegar decreased spiking activity of neurons expressing *Sfla Or67b1* (Fig. 3*B*; FDR adjusted $p<0.05$).

Although neurons expressing any of the *Sfla Or67b* paralogs responded to mustard plant volatiles, they differed in their responsiveness. Stimulation with arugula volatiles, for instance, elicited stronger responses in neurons expressing *Sfla Or67b1* (64 ± 7.8 spikes/sec; average ± SE) than in neurons expressing *Sfla Or67b2* (24 ± 8.7 spikes/sec) or *Sfla Or67b3* (22.3 ± 2.3 spikes/sec) (Fig. 3*B*; Kruskal Wallis ANOVA, $p<0.005$, followed by post-hoc Tukey tests, $p<0.05$; n=6 in each group). In contrast, stimulation with horseradish volatiles produced stronger responses in neurons expressing *Sfla Or67b3* (32 ± 4.4 spikes/sec) than in *Sfla Or67b1* (8.75 ± 1.3 spikes/sec) or *Sfla Or67b2* (12.8 ± 2.3 spikes/sec) (Fig. 3*C*; Kruskal Wallis ANOVA, $p<0.005$, followed by post-hoc Dunn's tests, $p<0.05$; n=6-9 in each group). Taken together, these results demonstrate that *Dmel Or67b* and *Spal Or67b* are functionally similar and may represent the ancestral phenotype, while *Sfla Or67b* paralogs are divergent and tuned to mustard plant volatiles.

***S. flava Or67b* paralogs respond selectively to ITCs and have different molecular receptive ranges**

Upon herbivore damage, mustard plants release ITCs and nitriles in addition to green leaf volatiles (GLVs) (32). In order to elucidate which odorants mediate activation of *Sfla* Or67b proteins, we tested a panel of 44 odorants which include ITCs, nitriles, GLVs, *Dmel* Or67b activators bearing various functional groups (33), and four ecologically relevant odorants which do not fall within these categories. Because many compounds were tested, for statistical comparisons we selected the odorants that produced the strongest average response across all Ors within each of the six chemical categories tested (those were butyl ITC, mandelonitrile, cis-3-hexenyl butyrate, trans-2-pentenal, and geranyl acetate (Fig. 3*A* and *C*). Neurons expressing any of the three *S. flava* paralogs responded to stimulation with butyl ITC ($p<0.05$), but not to stimulation with acetophenone ($p>0.1$; Fig. 3*A* and *C*). Conversely, acetophenone evoked the strongest excitatory responses from neurons expressing *Dmel Or67b* and *Spal Or67b* (respectively 175.7 ± 17.6 and 78 ± 15.2 spikes/second; average ± SE), while butyl ITC evoked no responses from neurons expressing *Dmel Or67b* ($p>0.5$), and only produced a slight increase in spiking activity (15 ± 4.2 spikes/second; average ± SE; $p<0.05$) from neurons expressing *Spal Or67b*.

***S. flava* Or67b1 and Or67b3 differ in their odor selectivity**

Although all *S. flava* paralogs are narrowly tuned to ITCs, they differ in their degree of selectivity and sensitivity. Butyl ITC evoked strong responses in neurons expressing *Sfla Or67b1* and *Or67b3* (196.3 ± 15.2 and 170.6 ± 11.2 spikes/second; average ± SE) that were not different from each other (Kruskal-Wallis ANOVA followed by Dunn's tests; $p>0.05$), while stimulation

with this odorant produced only a modest response from neurons expressing *Sfla Or67b2* (26.7 ± 2.8 spikes/second; Dunn's tests, in both cases $p<0.05$). None of the 44 odorants tested evoked strong responses from neurons expressing *Sfla Or67b2*, but it is possible that other compounds not tested in this study, and in particular mustard plant volatiles (Fig. 3*C*), activate this receptor.

Next, because ITCs are naturally diverse (34), we hypothesized that a particular subset of ITCs differentially activate *Sfla* Or67b1 and *Sfla* Or67b3. In order to test this, we stimulated neurons expressing *Sfla Or67b1* and *Or67b3* with various concentrations of six ITCs (3-methyl-thio-propyl ITC, butyl ITC, isobutyl ITC, sec-butyl ITC, benzyl ITC, and phenethyl ITC) that evoked very strong responses (>123 spikes/second) from neurons expressing *Or67b3* at 1:100 vol/vol (Fig. S4). At that concentration, only half of these odorants (3-methyl-thio-propyl ITC, butyl ITC, isobutyl ITC, and benzyl ITC) produced moderate to strong responses (41-147 spikes/second, depending on the odorant) from neurons expressing *Sfla Or67b1* (Fig. S4). At 1:1,000 vol/vol, the responses of *Sfla* Or67b3 to stimulation with phenethyl ITC, sec-butyl ITC and butyl ITC were different from those of *Sfla* Or67b1 (Mann-Whitney U tests corrected for multiple comparisons, FDR-adjusted p-values<0.05 in all cases; Fig. S4). Thus, although both *Sfla* Or67b1 and Or67b3 are highly selective and sensitive to ITCs, they have distinct odorant receptive ranges: *Sfla* Or67b3 is broadly tuned and strongly responds to all ITCs tested, while *Sfla* Or67b1 has a narrower receptive range and responds strongly only to a smaller subset of ITCs.

Or67b response relatedness, specificities, and functional evolution

We next compared the responses of all the Or67b proteins to all 44 odorants tested in a multi-dimensional space using principal component analysis (Fig. 4*A*). Each dot in Figure 4A

shows the vectors quantifying the control-subtracted odor responses of each Or67b copy plotted along the dimensions of the first three principal components, which captured 63.1%, 26.0%, and 9.0 % of the variance of the original high-dimensional data set. This analysis shows that: 1) most of the ITCs cluster separately from the other odorants tested, contributing to most of the variance (PC1) of the data set; 2) some *Dmel* activators and GLVs such as acetophenone and cis-3-hexenyl-butyrate also produced distinct responses, contributing largely to the variance of PC2; and 3) ITCs that activate *Sfla* Or67b1, such as sec-butyl ITC (but not butyl ITC) contribute to the variance of PC3. We also constructed tuning curves for each Or67b protein (Fig. 4*B*). The strongest responses (center of the distribution) from *Dmel* Or67b and *Spal* Or67b were evoked by *Dmel* activators and GLVs, while the strongest responses from all *Sflava* Or67b paralogs were evoked by ITCs. *Sfla* Or67b1 is particularly narrowly tuned to a few ITCs, as revealed by the high kurtosis value of the distribution (Fig. 4*B*). Then we conducted a neighbor joining cluster analysis based on the Euclidean distances between the odor-evoked responses from all the Ors. Among the *S. flava* paralogs, Or67b1 and Or67b3 have the most similar (shorter Euclidean distance) odorant responses (Fig. 4*C*).

Activation of *S. flava* Or67b1 and Or67b3 requires the presence of the ITC functional group

The finding that *Sfla* Or67b1 and *Sfla* Or67b3 respond to ITCs suggest that both the presence of the ITC functional group (–N=C=S) and the size of the molecule determine binding specificity. These two factors are indeed important to evoke responses from TrpA1, a non-selective electrophile chemoreceptor that relies on ligand-directed covalent modification (10). We thus asked whether this is also the case for *Sfla* Or67b1 and *Sfla* Or67b3, by testing their

responses to eleven electrophiles (non-ITCs) which activate TrpA1 by forming covalent linkages with sulfhydryl side chains. Interestingly, none of the non-ITC electrophiles activated neurons expressing *Sfla Or67b1*, and among these, only trans-2-pentenal produced a very small increase in spike activity (4 ± 1.3 spikes/second) from neurons expressing *Sfla Or67b3* (Fig. 3*C*). Additionally, we found that neurons expressing *Sfla Or67b* can respond to odor pulses that are seconds apart (Fig. S5). Because recovery from ligand-induced covalent modifications takes at least several minutes (and often hours) (7), these results suggest that activation of *Sfla* Or67b1 and Or67b3 by ITCs does not rely on the TrpA1-like covalent modification strategy.

We next investigated whether the presence of the ITC functional group (–N=C=S) is necessary for determining the responses of *Sfla* Or67b1 and *Sfla* Or67b3. In order to test this, we compared the responses of these Ors to benzyl ITC (BITC) and benzyl thiocyanate (-S≡C-N: BTC) (Fig.4*B*), linkage isomers that have the same molecular weight. We found that BITC produced robust activity in neurons expressing *Sfla Or67b1* or *Sfla Or67b3* (Mann-Whitney U tests, in both cases $p<0.002$), while BTC had little or no effect (Fig. 3*C* and 4*B*). This differential activation pattern is likely due to the differences in the functional group because BITC and BTC are not only isomers, but also have similar volatilities. These findings are consistent with the hypothesis that *Sfla* Or67b1 and *Sfla* Or67b3 detect ITCs by interacting with the ITC (–N=C=S) functional group selectively.

S. flava Or67b3 **is sufficient to induce olfactory attraction to ITCs**

Because *Sfla* Or67b paralogs, but not the orthologs from *Spal* and *Dmel*, specifically respond to ITC compounds, we asked whether these receptors can mediate olfactory attraction to these odor compounds. We focused on *Sfla* Or67b3, because this Or has a broader sensitivity to

ITCs than *Sfla* Or67b1 (Fig. 4*B*). We investigated this by testing the behavioral responses of *D. melanogaster* "empty neuron" mutants that expressed *Sfla Or67b3* or *Dmel Or67b* in the ab3A neuron. As before, we used a dual-choice "Y-shaped" olfactometer offering an odorant stimulus (butyl ITC 1:100 or 1:1,000 vol/vol) in one of the arms, and the solvent control in the other arm. We found that at the 1:100 vol/vol concentration of butyl ITC the odor responses of flies expressing *Sfla Or67b3* or *Dmel Or67b3* in the ab3A neuron were different from the 50% random expectation (two-tailed Binomial tests, $p<0.005$ and $p<0.01$ respectively), with flies orienting towards the odor in ca. 70-71% of tests (Fig. 5). In contrast, at the lowest odor concentration (1:1,000 vol/vol), the odor responses of flies expressing *Sfla Or67b3* -but not that of those expressing *Dmel Or67b*- in the ab3A neuron were different from the 50% random expectation (two-tailed Binomial tests, $p<0.00005$), with flies choosing the odorous side of the maze in 83% of tests (Fig. 5). Moreover, at the lower concentration, the odor-responses of flies expressing the *S. flava* transgene were different from those of flies expressing the *Dmel* transgene (Fisher Exact test, $p<0.05$). None of the three genetic control *Dmel* lines showed a preference for either side of the maze (Binomial tests, $p>0.1$ in all cases), even at the 1:100 vol/vol concentration (Fig. 5, first three columns). These results demonstrate that *Sfla Or67b3* can confer odor sensitivity to ITCs that persists at low (1:1,000 vol/vol) concentrations in a fly that is otherwise not attracted to these odor compounds.

Discussion

Plants have evolved a myriad of toxic "secondary" compounds to deter enemies which are generally perceived as noxious by animals (1). In spite of this, the vast majority of herbivorous insect species are specialized on one or a few host-plant lineages that contain

aversive compounds such as ITCs -the chemicals which give wasabi its characteristic pungent taste (35, 36). Through the course of evolution, specialist insects co-opted these chemicals as cues for host-finding, feeding, and egg laying (37). It is still unresolved, however, how attraction to these ancestrally aversive chemicals evolved. We addressed this gap using *S. flava*, a recently-derived herbivorous fly of mustard plants and their relatives (Brassicales). In behavioral experiments we found that *S. flava*, but neither of its microbe-feeding close relatives *S. pallida* or *D. melanogaster*, is attracted to mustard-plant volatiles, including volatile ITCs (Fig. 1). We next searched for changes in chemoreceptor proteins that could underlie this host plant-specific olfactory attraction. We found a candidate olfactory receptor gene (*Or67b*), which was triplicated in *S. flava*, resulting in three divergent and paralogous odorant receptor genes (*Sfla Or67b1-b3*; Fig. 2). These *Sfla Or67b* paralogs evolved with rates of amino-acid changing mutations that are consistent with episodic positive selection (Fig. 2*B*; TableS1). Next, using the 'empty neuron' system of *D. melanogaster*, we investigated the odor-response profiles of these odorant receptors. Consistent with our behavioral results, we found that two of the *Sfla* Or67b paralogs (*Sfla* Or67b1 and *Sfla* Or67b3) specifically respond to stimulation with mustard-plant odors and volatile ITCs (Fig. 3 and Fig S5). In contrast, *S. pallida* and *D. melanogaster* paralogs responded strongly to stimulation with apple cider vinegar and a broad range of aldehydes, alcohols and ketones (Fig. 3), consistent with their microbe-feeding habits. We also found that the presence of the ITC functional group is necessary for activation of *Sfla* Or67b and furthermore, that activation of the receptor likely does not involve a TrpA1-like covalent modification (Fig. 3, Fig. S4*C* (7)). Remarkably, when *Sfla Or67b3* was expressed in ab3A "empty neuron" system of *D. melanogaster*, adult female flies were attracted to butyl ITC in a y-maze assay (Fig. 5). This suggests that Or67b3 may be sufficient for the behavioral valence shift observed in the evolution

of mustard-feeding *Scaptomyza*, when expressed in novel neural circuit that ancestrally mediates attraction. Our results reveal the first Ors characterized from any animal that are tuned to mustard oils, and illustrate an evolutionary mechanism by which mustard specialists can evolve attraction towards otherwise aversive chemical compounds.

The gene triplication event that occurred in the *S. flava* lineage raises several interesting molecular evolutionary questions. Gene duplication plays an important role in evolutionary innovation (38) and several outcomes have been proposed regarding to how gene duplication contributes to acquisition of novel gene functions (38, 39): (A) neofunctionalization occurs when one of the two duplicated genes (paralogs) acquires a new function after accumulating *de novo* mutations, while the other copy retained its ancestral function; (B) subfunctionalization is largely considered a degenerative process whereby mutations accumulate in both copies, leading to partitioning of the ancestral function between the two gene copies; (C) specialization occurs when subfunctionalization and neofunctionalization evolve simultaneously, yielding gene copies that are "functionally distinct from each other and from the ancestral gene" (40, 41). The specialization model is supported by our data, as neither of the two outgroup Or67b proteins (*Spal* Or67b and *Dmel* Or67b) responded to ITCs (neofunctionalization), coupled with the fact that *Sfla* Or67b1 has a narrower breadth of tuning to ITCs than *Sfla* Or67b3 (subfuctionalization). Our conceptual model for this evolutionary hypothesis (Fig. 5) is that the ancestral Or67b ("1") was broadly tuned to acetophenone, alcohols and ketones, and diverged into a mustard oil-specific Or67b ("2") which lost sensitivity to these compounds and gained responsiveness to ITCs in the *S. flava* lineage. This *Or* triplicated during the course of evolution, ultimately giving rise to three Ors with different odor selectivity: (a) *Sfla* Or67b3, which retained broad sensitivity to ITCs; (b) *Sfla* Or67b1, which become narrowly tuned to a subset of *Sfla*

Or67b3 activators; and (c) *Sfla* Or67b2, which lost sensitivity to a broad range of ITCs (at least all the nine ITC compounds tested here) and likely retained or gained sensitivity to untested compounds.

Across *Drosophila*, orthologous chemoreceptors respond in a species-specific manner to ecologically relevant ligands. The best-studied of these is *Or22a*, which has been evolutionarily lost by gene deletion in *S. flava* but not in *S. pallida (19)*. In several drosophilids, Or22a is tuned to different ecologically relevant esters: ethyl-hexanoate in *D. melanogaster* (16), methyl-hexanoate in *D. sechellia* (42), 3-methyl-2-butenyl acetate in *D. erecta* (17), and isobutyl acetate in *D. suzukii* (43). Similarly, Ir75b is respectively tuned to butyric acid in *D. melanogaster* and to hexanoic acid in *D. sechellia* (15). Thus, host-specialization evolved in concert with the subtle re-sculpting of odor receptor selectivity associated with the ecological niche of *S. flava* (Fig. 6*b*). The fact that the chemical classes are still conserved for each chemoreceptor (i.e. esters in the case of Or22a and acids in the case of Ir75b), suggests that the chemical niche space and underlying sensory mechanisms are relatively conserved among species. In contrast, while *Spal* Or67b and *Dmel* Or67b specifically respond to alcohols, aldehydes and ketones, *Sfla* Or67b1 and *Sfla* Or67b3 respond selectively to volatile ITCs, thus acquiring a previously undescribed sensitivity to an entirely new chemical compound class (Fig. 6*b*). We hypothesize that the striking difference between Or67b-activating ligands among these species resulted from the dramatic niche shift -from feeding on microbes to feeding on live mustard plant tissue- that occurred in the evolution of herbivorous *Scaptomyza* that specialize on Brassicales plants.

TrpA1, which mediates taste-aversion to ITCs, is one of the most well-studied chemoreceptors (7, 8, 10). However, volatile ITCs are widely used to trap agricultural pests of Brassicales (4), and in agreement with this, the antennae of some of these insects respond to

these volatiles (44). Our study further advances our understanding of how volatile ITCs may be detected by these insects, by revealing Ors tuned to these chemical compounds. Furthermore, we uncovered an evolutionary mechanism, gene duplication followed by neofunctionalization and subfunctionalization, by which ITC-responsive Ors evolved in Brassicales specialists. More generally, our results suggest that major host shifts and specialization events in herbivorous insects can result from relatively simple genetic changes of large effect on the peripheral nervous system, similar to the apple maggot fly *Rhagoletis pomonella* (45). This in turn may explain why such events are so common across herbivorous insect lineages, resulting in rapid rates of diversification and leading to the most diverse guild of macroscopic life (46, 47).

Material and Methods:

Material and methods are summarized below. For complete details, see Supplemental Methods.

Fly lines

M2-MD refers to a CRISPR/Cas9-mediated deletion of *Or22a/b* and a knock-in of *Gal4* and *DsRed* by homologous repair. *Gal4* is not functional but *DsRed* is expressed in the eye. The functional absence of *Or22a* and *Or22b* genes in M2-MD flies was confirmed by electrophysiological analysis on *Or22a/b* expressing neurons in wild-type flies (Fig. S3). The four *UAS-Or67b* lines created in this study, the *UAS-Dmel Or67b* line, and the *UAS-dTrpA1* (stock no. 26264) line was each crossed into the M2-MD line. The progeny were then used for SSR recordings and behavioral experiments.

Behavioral tests of olfactory attraction

The olfactory responses of mated, non-starved *D. melanogaster* (Canton-S or transgenic), *S. pallida*, and *S. flava* were tested using a dual-choice "Y-shaped" olfactometer based on one previously published (20). Insects could walk upwind towards the "decision point" (intersection of the short and long arms of the "Y") and turn towards either the odor-laden or the odorless arm of the maze. Airflow was 250 ml/min in each arm of the maze. Four insects were released at once (to increase experimental efficacy), but only the first choice was considered. Each tested lasted a maximum of five minutes.

The odorants (20 µl of 1:100 vol/vol mineral oil solution) used in experiments were butyl ITC (Sigma-Aldrich, 592-82-5, USA) and sec-butyl ITC (Sigma-Aldrich, 15585-98-5, USA). For tests with transgenic flies, responses were tested at 1:100 vol/vol and 1:1,000 vol/vol of butyl ITC. We also used apple cider vinegar (40 µl, O Organics, USA; 40 µl of distilled water was as control stimulus in these tests). For tests of host orientation, two-four leaves from young arugula plants grown in an insect and insecticide/pesticide free chamber or greenhouse were excised just before tests, and placed in 5-ml syringes connected to the Y-maze.

For each odor/odorant, species, sex and genotype, the number of tests with insects orienting towards the odorous arm and the odorless arm of the Y-maze was used to conduct two-tailed Binomial tests (48). P-values were adjusted for multiple testing/comparisons using the false discovery rate method of Benjamin-Hochberg (49); results were considered statistically significant if the Benjamini-Hochberg adjusted p-value was <0.05. For all tests, we verified that the power was >0.8.

Molecular phylogeny of drosophilid odorant receptors:

Translations of *Ors* from *D. grimshawi*, *D. mojavensis, D. virilis* and *D. melanogaster* (builds dgri r1.3, dmoj r1.3, dvir r1.07 and dmel r6.28, respectively) were downloaded from Flybase (www.flybase.org, (50)) and *S. flava* sequences were obtained from ref. (19). Three hundred and nine sequences were aligned in MAFFT v7.017 with the E-INS-I algorithm and then manually adjusted (51). Models were fitted to the alignment using IQ-Tree and tested using the AIC criterion (52). A maximum likelihood (ML) phylogeny was generated using the Or protein alignment in RAxML v8.2.10 with the CAT model of rate heterogeneity with seven distinct categories, the JTT substitution matrix, empirical amino acid frequencies, and 1000 rapid boostraps (53). Orco sequences were designated as the outgroup.

Molecular phylogeny of drosophilid *Or67b* genes:

Or67b CDS from *D. grimshawi*, *D.* mojavensis*, D. virilis D. sechell b ia, D. simulans*, *D. erecta, D. yakuba, D. pseudoobscura, D. persimilis, D. ananassae, D. willistoni* and *D. melanogaster* (builds dgri r1.3, dmoj r1.3, dvir r1.07, dsec r1.3, dsim r1.4, dere r1.3, dyak r1.3, dpse r3.2, dper r1.3, dana r1.3, dwil r1.3 and dmel r6.28, respectively) were downloaded from Flybase (www.flybase.org, (50)). The *S. pallida* DNA sequence was obtained through PCR (*SI Appendix*, *Supplemental Methods*). Sequences were aligned, models fitted and chosen according to AIC (GTR+I+G) in IQ-Tree (52). Trees were inferred using RAxML (v8.2.10) with the GTRCATI model and 1000 rapid bootstraps, and MrBayes (v3.2.6) setting Nst to 6, nucmodel to 4by4, rates to Invgamma, number of generations to 125,000, burnin equal to 20% of generations, heating to 0.2, number of chains to 4, runs to 2 and priors set to default setting (54).

Analysis of molecular evolution:

CDS of homologs of every *Or* gene in *S. flava* found in the 12 *Drosophila* genome builds were aligned to *S. flava Or* CDS. Homology was assessed according to inclusion in well supported clades in the *Or* translation phylogeny above. Sequences were aligned in MAFFT (v7.017) (51) and adjusted manually to preserve codon alignments. Phylogenies were generated for every alignment using PhyML (55) with the GTR+G substitution models. If these trees showed >70% bootstrap support for a topology contrary to the known species topology, or if the Or homology group contained duplicates, these trees were used in PAML analyses instead of the species tree. Branch models of sequence evolution were fit using PAML 4.9h (26). A foreground/background branch model was fit for every *S. flava* tip branch and every ancestral branch in a *Scaptomyza*-specific *Or* gene duplication clade, and compared in a likelihood ratio test to a null model with one d*N*/d*S* rate for every unique phylogeny (total: 75 tests). After focusing on *Or67b*, patterns of molecular evolution among the drosophilid *Or67b* homologs were explored using the expanded *Or67b* CDS phylogeny above. Foreground/background branch models were fit for every branch in the *Or67b* phylogeny with identical likely ratio tests performed as above (29 tests total Fig. 2*B*; Table S1). P-values were adjusted for multiple testing using the FDR method (49).

Distance tree based on SSR recordings from neurons expressing *Or67b* transgenes

A matrix of average responses from five *Or67b* transgene receptors to 44 odorant compounds (1:100 vol/vol concentration) was produced (Table S3). Net responses were obtained by subtracting the response to mineral oil or dimethyl sulfoxide solvents. A Euclidean distance matrix was generated using the *dist* function from the R stats package (56). Receptor responses were clustered by using the neighbor joining (NJ) algorithm on this distance matrix. Support for

clusters was assessed using 1,000 bootstraps of the original response matrix by generating distance matrices and NJ trees on the pseudo-datasets in ape (v5.3) (57).

Single sensillum recordings (SSR)

Adult female flies were fed and then prepared for SSR as previously described (58). Extracellular activity was recorded by inserting a tungsten electrode into the base of the ab3 sensillum. The following odor sources (all purchased in Berkeley, California, US; 20 µl of material loaded on filter paper) were used: apple cider vinegar (O Organics, USA), grated roots of *Wasabia japonica* (wasabi), organic roots of *Armoracia rusticana* (horseradish), *Brassica rapa* (turnip), *Raphanus sativus* (daikon), and *Beta vulgaris* (beet). *Eruca vesicaria* (arugula) was grown from seeds in the lab, and leaves of 3-8 weeks old plants were used for odor stimulation. Roots or leaves were grated and homogenized using a vegetable grater to a volume equivalent to ~500 µl. The "net number of spikes" were obtained by counting the number of spikes during a 1-second window 0.2 seconds after the onset of stimulation, and subtracting from this number the background spiking activity (number of spikes during 1-second previous to the onset of odor stimulation). Data were analyzed using Mann-Whitney Rank sum tests (for comparisons involving two means) and p-values were adjusted for multiple comparisons using the FDR method, or by Kruskal-Wallis ANOVAs followed by Dunn's tests (for comparisons involving more than two means).

Data Analysis and figure generation:

All images and drawings are originals prepared by the authors. Figures were prepared via a combination of WinVDR (v3.8.5), R Studio (v1.2.1335), Microsoft Excel (2016), Adobe Illustrator (2019), Python, and Geneious (10.0.9).

Acknowledgments:

We are grateful to Drs. Chauda Sebastian, Dennis Mathew, John Carlson and Bloomington Drosophila Stock Center (NIH P40OD018537) for sharing *M2-MD*, *UAS-Dmel Or67b,* and *UAS-dTrpA1* (stock no. 26264), and to Drs. Johannes Bischof and Konrad Basler for donation of the pUASTattB plasmid. C.E.R. thanks Dr. Kristin Scott for support and encouragement. We thank members of the Whiteman and Scott Laboratories for discussions and comments on the manuscript. This work was supported by the National Institute of General Medical Sciences of the National Institutes of Health (award number R35GM119816 to N.K.W.) and the National Science Foundation (award number IOS 1755188 supporting B.G.-H.).

Figure Legends:

Figure 1: Olfactory behavioral responses of *S. flava* and its microbe-feeding relatives *S. pallida* and *D. melanogaster* to mustard oil volatiles and ITCs. (A) Schematic representation of the dual-choice maze used to test the olfactory responses of flies. One arm of the maze was connected to a 1-ml syringe containing a piece of filter paper loaded with an odorant (20 µl of a 1:100 vol/vol solution diluted in mineral oil) or apple cider vinegar (40 µl), while the other arm was connected to a syringe containing a piece of filter paper loaded with the control stimulus (20

µl of mineral oil or 40 µl of water). In the case of arugula, 2-4 leaves were excised from a plant just before tests and placed in a 5-ml syringe (the control syringe contained clean tissue paper). In each test a group of non-starved flies (n=4) was anesthetized in ice during 50-60 seconds and allowed to choose between the odor-laden or the odorless arm of the maze. Each test (maximum duration=5 min) ended when the first insect (out of the 4 released) made a choice for one or the other arm of the maze. The position of the odor-laden and odorless arm was alternated every 1-2 tests to control for potential spatial asymmetries. (B) Olfactory behavioral responses of *D. melanogaster*, *S. pallida* and *S. flava* to the odors and odorants indicated to the right. Data represent the proportion of tests in which insects choose the odorous arm of the maze, and the error bars indicate the 95% confidence interval of the proportion; the dotted reference line at 0.5 indicate no preference for the odorous or odorless arm of the maze. Numbers between parentheses indicate the number of tests with choices, either for the odorless or the odorous arm of the maze (on average, insects made a choice in 82% of the tests). For each fly species and odor, data was analyzed using two-tailed Binomial tests adjusted for multiple testing using FDR (adjusted p-values: * $p<0.05$, ** $p<0.01$, *** $p<0.005$, **** $p<0.001$). *S. flava* was attracted to mustard plant volatiles (arugula) and ITCs and avoided apple cider vinegar volatiles, while *S. pallida* avoided butyl ITC. *D. melanogaster* was attracted to vinegar but not to arugula volatiles or ITCs.

Figure 2: Maximum likelihood (ML) phylogeny of *Or67b*s in Drosophilidae. (A) ML phylogeny reconstructed from protein translations of the *Ors* found in *S. flava*, *D. melanogaster*, *D. grimshawi*, *D. virilis* and *D. mojavensis* genomes. Line width of branches are proportional to bootstrap support. Green branches indicate *Scaptomyza Ors*. Gene names with

bold fonts include branches with estimated d*N*/d*S* >1 from branch tests conducted in PAML, consistent with episodic positive selection. (B) ML phylogeny reconstructed from coding sequence of *Or67b* orthologs of twelve *Drosophila* species, *S. pallida* and *S. flava*. All bootstrap supports for the nodes are >80% and all posterior probabilities were >0.95 for the MrBayes tree. Branches with significant support (FDR p-value< 0.05) for d*N*/d*S* values different from the background rate are indicated with colored branch labels (blue where the foreground rate is less than the background, and red where d*N*/d*S* is greater than the background). Only *S. flava* and *D. mojavensis* branches have significantly elevated d*N*/d*S* according to branch model tests. *S. flava*, *S. pallida* and *D. melanogaster* branches are indicated by fly icons colored as in Figure 1. Scale bars are in units of substitutions per site.

Figure 3: Odor responses of orthologous and paralogous Or67b from *D. melanogaster*, *S. pallida* and S. *flava* to mustard-plant volatiles.

(A) *Or67b* paralogs and orthologs were expressed in a *D. melanogaster* mutant that lacks its endogenous *Or* (*Or22a*) in the ab3A olfactory receptor neuron (30). Shown is a representative trace of a single sensillum recording obtained from a *D. melanogaster* fly with *Dmel Or67b* expressed in the ab3A neuron (*Or22a*$^{-/-}$ *Or22b*$^{-/-}$; *Or22a-Gal4/UAS-Dmel Or67b*) (top left). Recordings from the ab3 sensilla produced spike trains from the two olfactory receptor cells housed within this sensilla (ab3A, which expresses *Or67b*, and ab3B, which expresses the native *Or85b*) that had distinct spike amplitudes. The ab3A neuron (labeled A) produced spikes of larger amplitude than the ab3B neuron (labeled B). Scale bar: 10 mV. Representative electrophysiological recordings obtained from the ab3 sensilla of flies expressing *Dmel Or67b*, *Spal Or67b*, *Sfla Or67b1*, *Sfla Or67b2* or *Or67b3* in the ab3A neuron in response to stimulation

with acetophenone, butyl ITC, sec-butyl ITC and mineral oil (solvent control). The bars below records indicate the onset and duration (1 sec) of the odor stimulation. Calibration bars: 10 mV. (B) Responses (net number of spikes/second; average ± SE, n= 6-8 sensilla obtained from 2-4 females) evoked by stimulation with apple cider vinegar, mustard plant volatiles and non-mustard plant volatiles (beet, control). Asterisks indicate significant differences between the responses to stimulation with an odor and the control stimulus (beet) (Mann-Whitney U tests corrected for multiple comparisons using FDR; adjusted p-values: * $p<0.05$; ** $p<0.01$; *** $p<0.005$). Note that neurons expressing *Dmel Or67b* and *Spal Or67b*, but not those expressing any of the *S. flava Or67b* paralogs, respond to apple cider vinegar. Conversely, only neurons expressing *S. flava Or67b* paralogs respond to mustard plant volatiles; neurons expressing *Sfla Or67b3* responded to all mustard plant volatiles tested. (C) Responses (net number of spikes/sec; average ± SE, n= 6-20 for each odorant, n=6-15 for mineral oil, obtained from 2-7 females) evoked by stimulation with single odorants categorized as follows: *Dmel* Or67b activators (Database of Odor Responses, Munch and Galizia 2016; orange), ITCs (green), nitriles (blue), green leaf volatiles (GLVs, purple), electrophiles/*TrpA1* activators (pink), other odorants not belonging to any of the previous categories (gray), and the two solvent controls (black). The responses of the strongest activator within each category (acetophenone, butyl ITC, mandelonitrile, cis-3-hexenyl butyrate, trans-2-pentenal, and geranyl acetate) were compared against the mineral oil control. Asterisks indicate significant differences between the responses to stimulation with each of these odorants and the control stimulus (statistics as described in B). Note that ITCs strongly activate neurons expressing *Sfla Or67b1* or *Sfla Or67b3*, and that for the most part these Ors do not respond to any of the other odorants tested. Some ITCs, such as sec-butyl ITC and phenethyl ITC, only activated neurons expressing *Sfla Or67b3*. *Spal Or67b* has an

odorant response profile similar to that of *Dmel Or67b*, responding mostly to stimulation with *D. melanogaster* activators and GLVs.

Figure 4: Or67b orthologs and paralogs have distinct and non-overlapping odor-response profiles, tuning breadths, and functional relatedness. (A) Vectors quantifying the odor-evoked responses (control-subtracted) were projected onto a two-dimensional subspace determined by the first three principal components of the data-set (left: PC1 vs PC2; right: PC1 vs PC3). PC1-3 captured each 63.1%, 26.0%, and 9.0% of the variances of the original five-dimensional data. Each dot represents one odorant, and the different colors and symbols indicate different chemical categories (as in Figure 3C and in the inset, right graph). (B) Tuning curves of each Or67b copy, showing the distribution of mean responses (n= 6-20) to the 44 odorants tested (color-coded as in A). The odorants are displayed along the horizontal axis according to the responses (net spikes/sec) they elicit from each Or. The odorants eliciting the strongest responses for each Or are located at the center of the distribution, while weaker activators are distributed along the edges of the distribution. Thus, the order of the odorants is different for the five Ors. Note that the strongest responses (center of the distribution) from *Dmel* Or67b and *Spal* Or67b are evoked by *D. melanogaster* activators and GLVs, while the strongest responses from all *Sfla* Or67b paralogs are evoked by ITCs. The tuning breadth of each Or is quantified by the kurtosis value (k) of the distribution with higher values indicating narrower odor-response profiles. The chemical structure of the top six *Sfla* Or67b3 activators and benzyl thiocyanate (numbers in green) are indicated to the right. (C) Neighbor joining cluster analysis for the five Or67b orthologs based on the Euclidean distances between the odor-evoked responses of the receptors.

Dmel Or67b and *Spal* Or67b are consistently separated from the *S. flava* odor response profiles, and *Sfla* Or67b1 and *Sfla* Or67b3 are consistently joined, having similar response profiles.

Figure 5: *S. flava Or67b3* confers olfactory attraction to ITCs

The responses of *D. melanogaster* flies expressing *Dmel Or67b* or *Sfla Or67b3* under the control of *Gal4* in the "empty" neuron (ab3A neuron) and three control parental lines were conducted as described in the caption to Figure 1. Genotypes are indicated at the bottom. One arm of the maze was connected to a 1-ml syringe containing a piece of filter paper loaded with 20 µl of 1:100 vol/vol (gray circles) or 1:1,000 vol/vol (black rectangles) of butyl ITC, while the other arm was connected to a syringe containing a piece of filter paper loaded with 20 µl of mineral oil. Data represent the proportion of tests in which insects choose the odorous arm of the maze; the deviation bars indicate the 95% confidence interval of the proportion. The dotted reference line at 0.5 indicate no preference for either arm of the maze; the numbers between parenthesis indicate the number of tests with choices for one or the other arm. Control flies (first three columns) showed no preference for either arm of the maze, even when tested with the highest concentration of butyl ITC (two-tailed Binomial tests, in all cases $p>0.1$). Note that flies carrying the *UAS-Sfla Or67b3* transgene under the control of *Gal4* in the ab3A neuron were attracted to both concentrations of butyl ITC (two-tailed Binomial tests, *** $p<0.005$; **** $p<0.001$). In contrast, flies carrying the *UAS-Dmel Or67b* transgene under the control of *Gal4* were attracted only to the highest concentration of the odorant (two-tailed Binomial tests, **$p<0.01$). At the lowest concentration, the response of flies carrying the *S. flava* transgene was different from the response of flies carrying the *D. melanogaster* transgene (Fisher Exact test, $p<0.05$). These

results thus indicate that in these flies, *Sfla Or67b3* is sufficient to confer attraction to butyl ITC which persist at low concentrations.

Figure 6: A model for the evolution of *Or67b* and comparison of tuning curves of orthologous Or22a, Ir75b and Or67b (A) The evolution of *Scaptomyza Or67b* begins with a shift in the tuning breadth and ligand specificity of an ancestral Or67b, from *Dmel* activators and GLVs to ITCs (neofunctionalization). Subsequent gene triplication of *Sfla Or67b* gave rise to three paralogous *Or67b* genes (*Sfla Or67b1, Sfla Or67b2,* and *Sfla Or67b3*). *Sfla* Or67b1 evolved to become more narrowly tuned, specializing in the detection of a few ITCs (subfunctionalization), while *Sfla* Or67b3 kept its ancestral, more broadly tuned state, responding to a broad range of ITCs. The ligands and tuning breadth of *Sfla* Or67b2 remain unresolved in this model. (B) The ligand specificities of orthologous Or22a, Ir75b, and Or67b. The Or22a orthologs from *D. melanogaster* (*Dmel* Or22a), *D. sechellia* (*Dsec* Or22a), *D. erecta* (*Der* Or22a), and *D. suzukii* (*Dsuz* Or22a) are all strongly activated by the host-derived esters indicated (top left;(16, 17, 42, 43)). The *Ir75b* orthologs from *D. melanogaster* (*Dmel Ir75b*), and *D. sechellia* (*Dsec Ir75b*) are strongly activated by the two acids indicated (top right; Prieto-Gordino et al. 2017(Prieto-Godino et al. 2017)). *Dmel* Or67b and *Spal* Or67b are strongly activated by acetophenone, while *Sfla* Or67b copies are activated by ITCs only (bottom). Note that Or22a and Ir75b orthologs are both divergent but activated by ligands belonging to a single chemical class (esters and acids, respectively). In contrast, the ligands of orthologous Or67b from *Dmel* and *Spal* are responsive to a variety of chemical classes which include alcohols, aldehydes and ketones, whereas *Sfla* Or67b orthologs are responsive to an entirely different chemical class (ITCs).

References:

1. G. Frankel, The raison d'etre of secondary plant substances. *Science* **129**, 1466–1470 (1959).

2. I. Winde, U. Wittstock, Insect herbivore counteradaptations to the plant glucosinolate–myrosinase system. *Phytochemistry* **72**, 1566–1575 (2011).

3. A. D. Gloss, *et al.*, Evolution in an ancient detoxification pathway is coupled with a transition to herbivory in the drosophilidae. *Mol. Biol. Evol.* **31**, 2441–2456 (2014).

4. A. Kergunteuil, S. Dugravot, A. Mortreuil, A. Le Ralec, A. M. Cortesero, Selecting volatiles to protect brassicaceous crops against the cabbage root fly, Delia radicum. *Entomol. Exp. Appl.* **144**, 69–77 (2012).

5. B. Al-Anzi, W. D. Tracey Jr, S. Benzer, Response of Drosophila to wasabi is mediated by painless, the fly homolog of mammalian TRPA1/ANKTM1. *Curr. Biol.* **16**, 1034–1040 (2006).

6. T. Ohta, T. Imagawa, S. Ito, Novel agonistic action of mustard oil on recombinant and endogenous porcine transient receptor potential V1 (pTRPV1) channels. *Biochemical Pharmacology* **73**, 1646–1656 (2007).

7. L. J. Macpherson, *et al.*, Noxious compounds activate TRPA1 ion channels through covalent modification of cysteines. *Nature* **445**, 541–545 (2007).

8. K. Kang, *et al.*, Analysis of Drosophila TRPA1 reveals an ancient origin for human chemical nociception. *Nature* **464**, 597–600 (2010).

9. O. M. Arenas, *et al.*, Activation of planarian TRPA1 by reactive oxygen species reveals a conserved mechanism for animal nociception. *Nat. Neurosci.* **20**, 1686–1693 (2017).

10. A. Hinman, H.-H. Chuang, D. M. Bautista, D. Julius, TRP channel activation by reversible covalent modification. *Proc. Natl. Acad. Sci. U. S. A.* **103**, 19564–19568 (2006).

11. R. M. Joseph, J. R. Carlson, Drosophila Chemoreceptors: A Molecular Interface Between the Chemical World and the Brain. *Trends in Genetics* **31**, 683–695 (2015).

12. C. Gomez-Diaz, F. Martin, J. M. Garcia-Fernandez, E. Alcorta, The Two Main Olfactory Receptor Families in Drosophila, ORs and IRs: A Comparative Approach. *Front. Cell. Neurosci.* **12**, 253 (2018).

13. A. Sanchez-Gracia, F. G. Vieira, J. Rozas, "Molecular evolution of the major chemosensory gene families in insects. Heredity (Edinb). 2009; 103 (3): 208-16" (Epub 2009/05/14. doi: 10.1038/hdy. 2009.55. PubMed PMID: 19436326).

14. P. Brand, S. R. Ramírez, The Evolutionary Dynamics of the Odorant Receptor Gene Family

in Corbiculate Bees. *Genome Biol. Evol.* **9**, 2023–2036 (2017).

15. L. L. Prieto-Godino, *et al.*, Evolution of Acid-Sensing Olfactory Circuits in Drosophilids. *Neuron* **93**, 661–676.e6 (2017).

16. S. Mansourian, *et al.*, Wild African Drosophila melanogaster Are Seasonal Specialists on Marula Fruit. *Curr. Biol.* **28**, 3960–3968.e3 (2018).

17. J. Linz, *et al.*, Host plant-driven sensory specialization in Drosophila erecta. *Proc. Biol. Sci.* **280**, 20130626 (2013).

18. N. K. Whiteman, *et al.*, Mining the plant-herbivore interface with a leafmining Drosophila of Arabidopsis. *Mol. Ecol.* **20**, 995–1014 (2011).

19. B. Goldman-Huertas, *et al.*, Evolution of herbivory in Drosophilidae linked to loss of behaviors, antennal responses, odorant receptors, and ancestral diet. *Proc. Natl. Acad. Sci. U. S. A.* **112**, 3026–3031 (2015).

20. C. E. Reisenman, Y. Lee, T. Gregory, P. G. Guerenstein, Effects of starvation on the olfactory responses of the blood-sucking bug Rhodnius prolixus. *J. Insect Physiol.* **59**, 717–721 (2013).

21. C. P. Faucher, M. Hilker, M. de Bruyne, Interactions of carbon dioxide and food odours in Drosophila: olfactory hedonics and sensory neuron properties. *PLoS One* **8**, e56361 (2013).

22. L. W. Aurand, J. A. Singleton, T. A. Bell, J. L. Etchells, Volatile Components in the Vapors of Natural and Distilled Vinegars. *J. Food Sci.* **31**, 172–177 (1966).

23. F. J. Cousin, *et al.*, Microorganisms in Fermented Apple Beverages: Current Knowledge and Future Directions. *Microorganisms* **5** (2017).

24. A. D. Gloss, *et al.*, Evolution of herbivory remodels a Drosophila genome. *bioRxiv*, 767160 (2019).

25. C. S. McBride, J. R. Arguello, B. C. O'Meara, Five Drosophila genomes reveal nonneutral evolution and the signature of host specialization in the chemoreceptor superfamily. *Genetics* **177**, 1395–1416 (2007).

26. Z. Yang, PAML 4: phylogenetic analysis by maximum likelihood. *Mol. Biol. Evol.* **24**, 1586–1591 (2007).

27. T. S. Ha, D. P. Smith, A pheromone receptor mediates 11-cis-vaccenyl acetate-induced responses in Drosophila. *J. Neurosci.* **26**, 8727–8733 (2006).

28. D. J. Hoare, *et al.*, Modeling peripheral olfactory coding in Drosophila larvae. *PLoS One* **6**, e22996 (2011).

29. S. G. Chin, S. E. Maguire, P. Huoviala, G. S. X. E. Jefferis, C. J. Potter, Olfactory Neurons

and Brain Centers Directing Oviposition Decisions in Drosophila. *Cell Rep.* **24**, 1667–1678 (2018).

30. E. A. Hallem, J. R. Carlson, Coding of Odors by a Receptor Repertoire. *Cell* **125**, 143–160 (2006).

31. F. Gonzalez, P. Witzgall, W. B. Walker, Protocol for Heterologous Expression of Insect Odourant Receptors in Drosophila. *Front. Ecol. Evol.* **4**, 189 (2016).

32. A. A. Agrawal, N. S. Kurashige, A role for isothiocyanates in plant resistance against the specialist herbivore Pieris rapae. *J. Chem. Ecol.* **29**, 1403–1415 (2003).

33. D. Münch, C. G. Galizia, DoOR 2.0--Comprehensive Mapping of Drosophila melanogaster Odorant Responses. *Sci. Rep.* **6**, 21841 (2016).

34. S. F. Vaughn, M. A. Berhow, Glucosinolate hydrolysis products from various plant sources: pH effects, isolation, and purification. *Industrial Crops and Products* **21**, 193–202 (2005).

35. P. R. Ehrlich, P. H. Raven, BUTTERFLIES AND PLANTS: A STUDY IN COEVOLUTION. *Evolution* **18**, 586–608 (1964).

36. J. A. Depree, T. M. Howard, G. P. Savage, Flavour and pharmaceutical properties of the volatile sulphur compounds of Wasabi (Wasabia japonica). *Food Res. Int.* **31**, 329–337 (1998).

37. E. A. Bernays, Evolution of Feeding Behavior in Insect HerbivoresSuccess seen as different ways to eat without being eaten. *Bioscience* **48**, 35–44 (1998).

38. S. Ohno, The Enormous Diversity in Genome Sizes of Fish as a Reflection of Nature˙s Extensive Experiments with Gene Duplication. *Trans. Am. Fish. Soc.* **99**, 120–130 (1970).

39. H. M. Heidel-Fischer, *et al.*, An Insect Counteradaptation against Host Plant Defenses Evolved through Concerted Neofunctionalization. *Mol. Biol. Evol.* **36**, 930–941 (2019).

40. X. He, J. Zhang, Rapid subfunctionalization accompanied by prolonged and substantial neofunctionalization in duplicate gene evolution. *Genetics* **169**, 1157–1164 (2005).

41. R. Assis, D. Bachtrog, Neofunctionalization of young duplicate genes in Drosophila. *Proc. Natl. Acad. Sci. U. S. A.* **110**, 17409–17414 (2013).

42. T. Dekker, I. Ibba, K. P. Siju, M. C. Stensmyr, B. S. Hansson, Olfactory shifts parallel superspecialism for toxic fruit in Drosophila melanogaster sibling, D. sechellia. *Curr. Biol.* **16**, 101–109 (2006).

43. I. Keesey, *et al.*, Evolution of a pest: towards the complete neuroethology of Drosophila suzukii and the subgenus Sophophora. *BioRxiv* (2019).

44. J. A. A. Renwick, M. Haribal, S. Gouinguené, E. Städler, Isothiocyanates stimulating

oviposition by the diamondback moth, Plutella xylostella. *J. Chem. Ecol.* **32**, 755–766 (2006).

45. C. Tait, S. Batra, S. S. Ramaswamy, J. L. Feder, S. B. Olsson, Sensory specificity and speciation: a potential neuronal pathway for host fruit odour discrimination in Rhagoletis pomonella. *Proc. Biol. Sci.* **283** (2016).

46. J. J. Wiens, R. T. Lapoint, N. K. Whiteman, Herbivory increases diversification across insect clades. *Nat. Commun.* **6**, 8370 (2015).

47. C. Mitter, B. Farrell, B. Wiegmann, The Phylogenetic Study of Adaptive Zones: Has Phytophagy Promoted Insect Diversification? *Am. Nat.* **132**, 107–128 (1988).

48. J. H. Zar, *Biostatistical Analysis* (Prentice Hall, 1999).

49. Y. Benjamini, Y. Hochberg, Controlling the False Discovery Rate: A Practical and Powerful Approach to Multiple Testing. *Journal of the Royal Statistical Society: Series B (Methodological)* **57**, 289–300 (1995).

50. J. Thurmond, *et al.*, FlyBase 2.0: the next generation. *Nucleic Acids Res.* **47**, D759–D765 (2019).

51. K. Katoh, MAFFT: a novel method for rapid multiple sequence alignment based on fast Fourier transform. *Nucleic Acids Research* **30**, 3059–3066 (2002).

52. L.-T. Nguyen, H. A. Schmidt, A. von Haeseler, B. Q. Minh, IQ-TREE: A Fast and Effective Stochastic Algorithm for Estimating Maximum-Likelihood Phylogenies. *Molecular Biology and Evolution* **32**, 268–274 (2015).

53. A. Stamatakis, RAxML version 8: a tool for phylogenetic analysis and post-analysis of large phylogenies. *Bioinformatics* **30**, 1312–1313 (2014).

54. F. Ronquist, *et al.*, MrBayes 3.2: efficient Bayesian phylogenetic inference and model choice across a large model space. *Syst. Biol.* **61**, 539–542 (2012).

55. S. Guindon, *et al.*, New Algorithms and Methods to Estimate Maximum-Likelihood Phylogenies: Assessing the Performance of PhyML 3.0. *Systematic Biology* **59**, 307–321 (2010).

56. R. C. Team, R: a language and environment for statistical computing [online]. R Foundation for Statistical Computing, Vienna, Austria (2018).

57. E. Paradis, K. Schliep, ape 5.0: an environment for modern phylogenetics and evolutionary analyses in R. *Bioinformatics* **35**, 526–528 (2019).

58. E. A. Hallem, J. R. Carlson, The odor coding system of Drosophila. *Trends in Genetics* **20**, 453–459 (2004).

59. R. T. Lapoint, P. M. O'Grady, N. K. Whiteman, Diversification and dispersal of the Hawaiian Drosophilidae: the evolution of Scaptomyza. *Mol. Phylogenet. Evol.* **69**, 95–108 (2013).

60. J. Bischof, R. K. Maeda, M. Hediger, F. Karch, K. Basler, An optimized transgenesis system for Drosophila using germ-line-specific φC31 integrases. *Proc. Natl. Acad. Sci. U. S. A.* **104**, 3312–3317 (2007).

Supplemental Fig Legends:

Supplemental Fig. 1: Protein alignment of *D. melanogaster*, *S. pallida* and *S. flava* Or67bs.

Note the high number of identical amino acids across orthologs/paralogs (black squares). Also shown are each of the seven predicted transmembrane domains (TM1-7). Darker colors illustrate higher degrees of sequence similarity, and lighter colors denote residues with high variability in sequence across paralogs and orthologs.

Supplemental Figure 2: *Or67bs* are expressed in *Scaptomyza* spp.

A) Amplification of *Marf* from cDNA generated from whole body extracts of *S. flava* and *S. pallida* adults (+RT). As expected, *Marf* does not amplify in templates treated with DNaseI without reverse transcriptase (– RT). B) Amplification of *Or67b* genes from *S. pallida* and *S. flava* whole adult cDNA, indicative of *in vivo* transcription of *Or67b* genes in adult *Scaptomyza*. Ladder is Gene Ruler™ 1 kb plus (ThermoFisher).

Supplemental Figure 3: *Or22a* is not expressed in M2-MD line and dTrpA1 does not responsive to volatile electrophiles.

(A) Lack of *Or22a* expression in the ab3A neuron in the M2-MD fly line ("empty neuron" mutant) was verified by lack of electrophysiological responses to ethyl hexanoate (left). In contrast, in wild-type flies (Canton-S), ab3A neurons respond strongly to simulation with this odor compound (right). Data indicates the net number of spikes/sec (average ± SE, n= 6-7 for

each odor and control stimulation, obtained from 3 females). (B) Single odorants used for statistical analysis in Fig. 3 were tested on the mutant ab3A neuron lacking its endogenous olfactory receptor. Stimulation with any of the odorants failed to evoke spiking activity. (C) *dTrpA1* was expressed in the ab3A neuron in the M2-MD fly line. None of the volatile ITCs or electrophiles elicited spiking activity. For a list of odorant categories see Fig. 3.

Supplemental Figure 4: Odorant dose–responses of *Sfla* Or67b1 and *Sfla* Or67b3

Responses (net spikes/sec, average +/- SE, n=6, obtained from 2 animals) of *Sfla* Or67b1 and *Sfla* Or67b3 to stimulation with increasing concentrations (vol/vol) of six different ITCs. The responses of *Sfla* Or67b3 steadily increased with increasing the concentration of all ITCs tested. *Sfla* Or67b1 and *Sfla* Or67b3 showed similar dose-response relationships in response to stimulation with 3-methyl-thio-propyl-ITC, butyl ITC, and benzyl ITC. Stimulation with sec-butyl ITC and phenethyl ITC produced only a very slight increase in spike activity (<10 spikes/second) from *Sfla* Or67b1 at any of the concentrations tested. The asterisks indicate significant differences between the responses to the 1:1,000 vol/vol concentration and the responses to the mineral oil control (Mann-Whitney U tests corrected for multiple testing using FDR; adjusted p-values: * $p<0.05$, ** $p<0.01$, *** $p<0.005$).

Supplemental Figure 5: *Sfla* Or67b response recovers within seconds.

Representative electrophysiological recording obtained from the ab3 sensilla of flies expressing *Sfla Or67b3* in response to stimulation with iso-butyl ITC following sec-butyl ITC with one second interval between administration. The horizontal bar denotes one second and the vertical

bar denotes 10 mV. Note, *Sfla* Or67b3 response is recovered within seconds after stimulation with ITCs.

Supplemental Material and Methods:

Fly husbandry and lines

D. melanogaster (Canton-S) were reared using standard cornmeal media, yeast, and agar medium. Isofemale lines of *S. pallida* (collected in Berkeley, California, US) were maintained on Nutri-Fly medium (Genesee Scientific). *S. flava* (collected in New Hampshire, US) were maintained on fresh *Arabidopsis thaliana* and 10% honey water solution. All flies were cultured at 23°C and 60% relative humidity under a 12-h light/12-h dark cycle. *S. flava* and *S. pallida* were about 7-10 days old at the time of experiments; *D. melanogaster* (wild-type or transgenic) were about 3-10 days old at the time of the experiments.

M2-MD refers to a CRISPR/Cas9 deletion of *Or22a/b* and a knock-in of *Gal4* and *DsRed* by homologous repair. *Gal4* is not functional but *DsRed* is expressed in the eye. The functional absence of *Or22a* and *Or22b* genes in M2-MD flies was confirmed by electrophysiological analysis on *Or22a/b* expressing neurons in wild-type flies (Fig. S3). The M2-MD line was used to generate flies expressing *Dmel Or67b*, *Spal Or67b* and *Sfla Or67b1-3* under the control of *Gal4* in the ab3A "empty neuron". The *UAS-SflaOr67b1, UAS-Sfla Or67b2, UAS-Sfla Or67b3,* and *UAS-Spal Or67b* strains were generated during this study.

***Scaptomyza Or67b* gene cloning, UAS line generation, and verification of *S. flava Or67b* transcription**

The *UAS-Or67b* transgene lines were constructed as follows: RNA was extracted from 20–25 male and female, laboratory-reared, adult flies of *S. pallida* (collected from the White Mountains, New Mexico) and *S. flava* (collected from near Portsmouth, New Hampshire). RNA was extracted using Trizol (Thermo-Fisher, Waltham, MA) and precipitated with isopropanol. Extracted RNA was treated with DNaseI; cDNA was then generated using qScript cDNA Supermix (Quantabio, Beverly, MA). Absence of gDNA in cDNA preparations was verified by attempting to amplify fragments of the *Marf* gene from reactions lacking reverse transcriptase (Fig. S2; PCR conditions and primers detailed in (59)). CDS plus 7–9 bp of untranslated sequence were amplified using High Fidelity Phusion Taq (New England BioLabs, NEB), 3% DMSO v/v, and the PCR primers (Table S2) with the following program: initial denaturing at 98°C during 30 sec; 35 cycles at 98°C for 10 sec, 58°C for 30 sec, 72°C for 45 sec, and extension at 72°C during 7 min. PCR fragments of the expected size were purified using Qiaquick Gel purification kit protocol (Qiagen). An overhang was added to purified *Or67b* amplicons with Taq polymerase (Fermentas) and cloned using the pGEM-T Easy cloning kit protocol (Promega). Plasmids were extracted and purified using the GenElute plasmid miniprep kit (Sigma-Aldrich, St. Louis, MO). EcoRI and KpnI cut sites were introduced using restriction enzyme cut-site primers (Table S2) with 10 ng/µL diluted plasmids (as template) with 3% DMSO vol/vol and the following program: initial denaturing at 98°C for 30 sec; 35 repetitions of 98°C for 10 sec, 55°C for 50 sec; 72°C for 45 sec; and final extension at 72°C for 7 min. The pUAST attB plasmid (60) and the four *S. pallida* and *S. flava Or67b* PCR amplicons with RE flanking sites were individually double-digested with KpnI and EcoRI high-fidelity enzyme in

cut smart buffer for 3 hours, according to the manufacturer's protocol (NEB). Cut fragments were gel-purified using the Qiaquick Gel Cleanup Kit (Qiagen) and ligated in a 1:3 vector:insert molar ratio using T4 ligase (Promega). Ligations were transformed into JM109 cells. Some cells were preserved as glycerol stocks and a portion were sent for injection into the y^1 w^{67c23}; P{CaryP}attP2 fly line (BestGene Inc., Houston, Texas, USA). Transformants were selected from individually injected flies with eye color rescue phenotypes. The four *UAS-Or67b* lines created in this study, the *UAS-Dmel Or67b* line, and the *UAS-dTrpA1* (stock no. 26264) line was each crossed into the M2-MD line. The progeny were then used for SSR recordings and behavioral experiments.

Behavioral tests of olfactory attraction

The olfactory responses of mated, non-starved *D. melanogaster* (Canton-S or transgenic), *S. pallida*, and *S. flava* were tested using a dual-choice "Y-shaped" olfactometer based on one previously published (20). The "Y piece" of the olfactometer was a propylene connector (43 mm long x 60 mm); the open ends of the arms of the "Y" were each connected to a 1-ml syringe containing a piece of filter paper (600 x 50 mm) loaded with the odor or control stimuli. Charcoal-filtered air was delivered to each of the two syringes using silicon tubing at 250 ml/min; thus, at the base of the maze air flow was approximately 500 ml/min. Two hours (in the case of *D. melanogaster* and *S. pallida*) or 20 hours before tests (in the case of *S. flava*) insects were gently anesthetized under CO_2 and placed in groups of four in open-top and mesh-bottom cylindrical release containers (20 mm long x 10 mm diameter) constructed using silicon tube. The open top of the containers was capped with a piece of cotton soaked in distilled water (in the case of *D. melanogaster* and *S. pallida*) or with a piece of cotton soaked in 10% vol/vol aqueous

honey solution (in the case of *S. flava*). Before tests, each release tube was placed in ice during 45-60 seconds to slow down insect activity, the cotton cap was removed, and the open-top of the tube was carefully slid into the open end of the Y maze. Thus, upon being released, insects could walk upwind towards the "decision point" (intersection of the short and long arms of the "Y") and turn towards either the odor-laden or the odorless arm of the maze. Although four insects were released at once (to increase experimental efficacy), only the first choice (and the time of the choice) was recorded; a choice was considered as such only if the insect walked past at least 10 mm into one of the arms, orienting upwind. The test was discarded if two or more insects choose the two arms of the maze within a 3-second window of each other. Each test lasted a maximum of five minutes, and each group of insects was used only once. As much as possible, insects from the same cohort were tested in the same day with different odors/odorants; insects from the three different species were also, as much as possible, tested in the same day with a given odor/odorant/different fly genotypes. Tests with each species/stimulus were conducted in at least five different days to compensate for possible day-to-day variations. Results from an individual test session with a given odor/odorant were discarded if less than 50% of the insects made a choice (this happened in less than 5% of experimental sessions). The position of the odor and odorless arms was switched every 1-2 tests to control for positional asymmetries; the mazes and odor sources were changed and replaced for clean/new ones every four tests or 10 minutes, whichever comes first.

The odor/odorant was loaded in a piece of filter paper and inserted into the 1-ml syringe right before tests; control syringes had a piece of filter paper (3 x 40 mm) loaded with the mineral oil solvent (for odorant solutions) or water (for odor mixtures). Experimental and control filter papers were replaced by fresh ones every 4 tests or 10 minutes, whichever came first. The

odorants (20 µl of 1:100 vol/vol mineral oil solution) used in experiments were butyl ITC (Sigma-Aldrich, 592-82-5, USA) and sec-butyl ITC (Sigma-Aldrich, 15585-98-5, USA). For tests with transgenic flies, responses were tested at 1:100 vol/vol and 1:1,000 vol/vol of butyl ITC. We also used apple cider vinegar (40 µl, O Organics, USA; 40 µl of distilled water was as control stimulus in these tests). For tests of host-orientation, two-four leaves from young arugula plants grown in an insect and insecticide/pesticide free chamber or greenhouse were excised just before tests, and placed in 5-ml syringes connected to the Y-maze; control syringes had two pieces of tissue paper. In all cases the Y-mazes, tubing and syringes were cleaned with 70% ethanol and allowed to air-dry before reusing. Experiments were conducted during the 2nd-5th hour of the insects' photophase at 24 ºC under white light (Feit electric, 100 Watts; in the case of *S. pallida* and *D. melanogaster*) or green light (Sunlite green, 100 Watts; in the case of experiments with *S. flava*). A total of 1,061 (669 with wild-type flies of *D. melanogaster*, *S. pallida* and *S. flava*; 392 with transgenic *D. melanogaster*) tests were and insects made a choice in 84% (888) of tests.

For each odor/odorant, species, sex and genotype, the number of tests with the first insect orienting towards the odorous arm and the odorless arm of the Y-maze were tested against a 50% expected random distribution using two-tailed Binomial tests (48). P-values were adjusted for multiple comparisons using the false discovery rate (FDR) method of Benjamin-Hochberg (49); results were considered significant if the Benjamini-Hochberg adjusted p-value was <0.05. For all tests, we verified that the power was >0.8.

Molecular phylogeny of drosophilid Odorant Receptors (*Or*):

Translations of *Ors* from *D. grimshawi*, *D. mojavensis, D. virilis* and *D. melanogaster* (builds dgri r1.3, dmoj r1.3, dvir r1.07 and dmel r6.28, respectively) were downloaded from Flybase (www.flybase.org, (50)). *S. flava* sequences were previously published (19). Three hundred and nine sequences were aligned in MAFFT v7.017 with the E-INS-I algorithm and then manually adjusted (51). Models were fitted to the alignment using IQ-Tree and tested using the AIC criterion (52). A maximum likelihood (ML) phylogeny was generated using the Or protein alignment in RAxML v8.2.10 with the CAT model of rate heterogeneity with seven distinct categories, the JTT substitution matrix, empirical amino acid frequencies, and 1,000 rapid boostraps (53). Orco sequences were designated as the outgroup.

Molecular phylogeny of drosophilid *Or67b* genes:

Or67b CDS from *D. grimshawi*, *D. mojavensis, D. virilis D. sechellia, D. simulans*, *D. erecta, D. yakuba, D. pseudoobscura, D. persimilis, D. ananassae, D. willistoni* and *D. melanogaster* (builds dgri r1.3, dmoj r1.3, dvir r1.07, dsec r1.3, dsim r1.4, dere r1.3, dyak r1.3, dpse r3.2, dper r1.3, dana r1.3, dwil r1.3 and dmel r6.28, respectively) were downloaded from Flybase (www.flybase.org, (50)). The *S. pallida* DNA sequence was obtained through PCR as described above; *S. flava* DNA sequences were previously published (19). Sequences were aligned, models fitted and chosen according to AIC (GTR+I+G) in IQ-Tree (52). Trees were inferred using RAxML (v8.2.10) with the GTRCATI model and 1000 rapid bootstraps, and MrBayes (v3.2.6) setting Nst to 6, nucmodel to 4by4, rates to Invgamma, number of generations to 125,000, burnin equal to 20% of generations, heating to 0.2, number of chains to 4, runs to 2 and priors set to default setting (54).

Analysis of molecular evolution:

CDS of homologs of every *Or* gene in *S. flava* found in the 12 *Drosophila* genome builds were aligned to *S. flava Or* CDS. Homology was assessed according to inclusion in well supported clades in the *Or* translation phylogeny above; *S. flava* sequences were previously published (19). Sequences were aligned in MAFFT (v7.017) (51) and adjusted manually to preserve codon alignments. *Or98a*-like genes found in subgenus *Drosophila* species were split into three separate clades, as were a group of *Or83c* paralogs not found in *D. melanogaster*, and a group of *Or85a*-like genes. All sequences examined of *Or46a* contain two alternatively spliced exons, so this gene was analyzed with all gene exon sequences in a single alignment as single taxa. *Or69a*, however, contains alternatively spliced exons only among *Sophophora* species. These alternative splice forms were analyzed as separate taxa. Phylogenies were generated for every alignment using PhyML (55) with the GTR+G substitution models. If these trees showed >70% bootstrap support for a topology contrary to the known species topology, or if the Or homology group contained duplicates, these trees were used in PAML analyses instead of the species tree. Branch models of sequence evolution were fit using PAML 4.9h (26). A foreground/background branch model was fit for every *S. flava* tip branch and every ancestral branch in a *Scaptomyza*-specific *Or* gene duplication clade, and compared in a likelihood ratio test to a null model with one d*N*/d*S* rate for every unique phylogeny (75 tests total). After focusing on *Or67b*, patterns of molecular evolution among the drosophilid *Or67b* homologs were explored using the expanded *Or67b* CDS phylogeny above. Foreground/background branch models were fit for every branch in the *Or67b* phylogeny with identical likely ratio tests performed as above (29 tests total Fig. 2*B*; Table S1). P-values were adjusted for multiple-testing using the FDR method (49).

Distance tree obtained from responses of ab3A neurons expressing *Or67b* transgenes

A matrix of average response of five *Or67b* transgene receptors to 44 odorant compounds (1:100 vol/vol concentration) was produced (Table S3). Net responses were calculated by subtracting the response to mineral oil or dimethyl sulfoxide solvent from the odor-evoked responses. A Euclidean distance matrix was generated using the dist function of the R stats package(56). Receptor responses were clustered by using the neighbor joining (NJ) algorithm on this distance matrix. Support for clusters was assessed using 1000 bootstraps of the original response matrix by generating distance matrices and NJ trees on the pseudo-datasets in ape (v5.3) (57).

Single sensillum recordings (SSR)

Female fed flies were prepared for SSR as previously described (58). We identified sensilla of targeted olfactory receptor cells using an Olympus BX51WI upright microscope with 10x and 50x objectives (Olympus, UPlanFL N 10x, UPlanFL N 50x). Extracellular activity was recorded by inserting a tungsten electrode into the base of the ab3 sensillum. Signals were amplified 10,000 x (A-M systems, Differential AC Amplifier model 1700), digitized using a 16-bit analog-digital converter, filtered (low cut-off: 300 Hz, high cut off: 3k Hz), and analyzed off-line with WinEDR (v3.8.5; University of Strathclyde, Glasgow). A tube delivering a constant flow of charcoal-filtered air was placed near the fly's head, and the tip of the stimulation pipette (50 ml) was inserted into the constant air stream. The stimulation pipette contained a piece of filter paper loaded with 20 µl of odorant solution or the solvent control. One second pulse of clean air was delivered to the stimulus pipette using a Stimulus Controller CS 55 (Syntech, Germany). We used three standard odors for identification of ab3 sensilla (all from Sigma-Aldrich, US, purity > 1%): ethyl hexanoate (catalog # 123-66-0), ethyl acetate (catalog # 141-78-6) and 2-heptanone

(catalog # 110-43-0). The following odor sources (all purchased in Berkeley, California, US; 20 µl of material loaded on filter paper) were used: apple cider vinegar (40 µl, O Organics, USA), grated roots of *Wasabia japonica* (wasabi), organic roots of *Armoracia rusticana* (horseradish), *Brassica rapa* (turnip), *Raphanus sativus* (daikon), and *Beta vulgaris* (beet). *Eruca vesicaria* (arugula) was grown from seeds at 23°C and 60% relative humidity in a 12-hours light: 12-hours dark cycle, and leaves from 3-8 weeks old plants were used for odor stimulation. Roots and leaves were grated and homogenized using a vegetable grater to a volume equivalent to ~500 µl. The following odorants (all from Sigma-Aldrich, US) were diluted 1:100 vol/vol in dimethyl sulfoxide: iodoacetamide (catalog # 144-48-9), N-methylmaleimide (catalog # 930-88-1), N-hydroxysuccinimide (catalog # 6066-82-6), and 3-indol-carbinole (catalog # 700-06-1) and benzyl thiocyanate (catalog # 3012-37-1). All the other chemicals were diluted in mineral oil at 1:100, 1:1,000, and 10,000 vol/vol. The "net number of spikes" were obtained by counting the number of spikes during a 1-second window 0.2 seconds after the onset of stimulation, and subtracting from this number the background spiking activity (obtained by counting the number of spikes in a 1-second window prior to the onset of the odor stimulation). Data was analyzed using Mann-Whitney Rank sum tests (for comparisons involving two means) and p-values were adjusted for multiple comparisons using the FDR method, or by Kruskal-Wallis ANOVAs followed by Dunn's tests (for comparisons involving more than two means).

Principal Component Analysis (PCA). For visualization, Principal component analysis (PCA) was done using Python.

Data Analysis and figure generation:

All images and drawings are originals prepared by the authors. Figures were prepared via a combination of WinVDR (v3.8.5), R Studio (v1.2.1335), Microsoft Excel (2016), Adobe Illustrator (2019), Python, and Geneious (10.0.9).

Table S1: Parameters from Odorant Receptor molecular evolution analyses

Test*	Branch†	background dN/dS	foreground dN/dS	dN – dS	FDR adjusted p-value
OR	Or2a	0.10948	0.08368	-1.1523	0.4031933
OR	Or10a	0.16074	0.08826	-0.5837	**0.03599091**
OR	Or13a1	0.13815	0.95538	-0.0014	**8.36204E-06**
OR	Or13a2	0.14485	0.29386	-0.0114	0.5374215
OR	Or13a ancestor	0.1405	0.22696	-0.2232	0.1062494
OR	Or19a	0.27184	0.256	-0.3699	0.8337806
OR	Or22c	0.15572	0.25996	-0.1496	0.1475187
OR	Or23a	0.16331	0.2829	-0.2438	0.0934421
OR	Or24a	0.08324	0.09358	-0.5121	0.7036877
OR	Or30a	0.07027	0.10685	-0.4864	0.1396827
OR	Or33c	0.20981	0.15322	-0.402	0.2748754
OR	Or35a	0.10058	0.80581	-0.2963	**0.00245945**
OR	Or42a1	0.10806	0.11791	-0.336	0.7716366
OR	Or42a2	0.10578	0.80581	-0.012	**0.000970903**
OR	Or42a3	0.10571	0.80581	-0.0045	**0.000643469**
OR	Or42a2 and 3 ancestor	0.11046	0.08409	-0.5505	0.3637872
OR	Or43a	0.14775	0.08518	-0.3217	0.1557934
OR	Or45b	0.10067	0.10449	-0.3992	0.8803498
OR	Or46a	0.14313	0.20832	-0.2632	0.1151226
OR	Or47b	0.16957	0.15781	-0.3375	0.8025064
OR	Or49a	0.19774	0.17914	-0.5377	0.7036877
OR	Or49b	0.10784	0.05836	-0.3747	0.09592573
OR	Or56a	0.12598	0.05652	-0.5602	**0.004298517**
OR	Or59a	0.1085	0.31529	-0.2475	**0.000415309**
OR	Or59b	0.09936	0.23227	-0.4421	**0.000415309**
OR	Or63a1	0.12346	∞	**0.0172**	**3.51892E-05**
OR	Or63a2	0.12136	∞	**0.0274**	**1.35815E-09**
OR	Or63a ancestor	0.10903	0.56602	-0.1212	**5.0862E-13**
OR	Or67a1	0.20346	0.13116	-0.528	0.0934421
OR	Or67a2	0.2067	**0.06369**	-0.0693	**0.0004729**
OR	Or67b1	0.11719	0.87005	-0.0059	**2.5914E-07**
OR	Or67b2	0.11479	0.69462	-0.0253	**1.96849E-09**
OR	Or67b3	0.10844	**1.95161**	**0.0414**	**9.78045E-20**
OR	Or67b1 and 2 ancestor	0.11932	∞	**0.0282**	**3.90702E-08**
OR	Or67b1, 2 and 3 ancestor	0.11679	0.28275	-0.2591	**0.000585544**
OR	Or67c	0.05491	0.07255	-0.4886	0.4029281

OR	Or67d	0.12277	**7.22359**	**0.0948**	**2.56153E-05**
OR	Or69a	0.21665	0.12519	-0.4274	0.05279388
OR	Or71a	0.15846	0.25285	-0.3464	0.1151226
OR	Or74a1	0.13897	0.16825	-0.3766	0.5728869
OR	Or74a2	0.13723	0.18825	-0.4375	0.2932306
OR	Or82a	0.12569	0.18201	-0.2805	0.1926929
OR	Or83a	0.0967	0.13983	-0.4518	0.148133
OR	Or83c1	0.16267	0.21756	-0.4381	0.3145556
OR	Or83c2	0.22615	0.41682	-0.1561	0.0934421
OR	Or83c3	0.22488	0.39035	-0.2043	0.0934421
OR	Or83c2 and 3 ancestor	0.25561	0.17609	-0.2679	0.5410598
OR	Or85aLike	0.22488	0.39035	-1.8882	**0.001826812**
OR	Or85bc	0.19387	**0.07261**	-0.32	0.2783313
OR	Or85e	0.15034	0.20391	-0.3561	0.6592839
OR	Or85f	0.11206	0.13076	-0.4139	0.08611496
OR	Or88a	0.18031	0.09816	-0.2848	**0.003678095**
OR	Or92a	0.14147	0.32458	-0.3894	**3.51892E-05**
OR	Or94a	0.044	0.13816	-0.4616	0.1933
OR	Or94b	0.09284	0.14353	-0.5473	0.09592573
OR	Or98a1	0.09893	0.17168	**0.0013**	0.1796849
OR	Or98a3	0.18051	1.69406	-0.0093	0.6770641
OR	Or98a7	0.18219	0.28105	**0.0258**	**5.47517E-05**
OR	Or98a1 and 3 ancestor	0.14909	**2.74217**	-0.0113	**0.00014207**
OR	Or98a1, 3 and 7 ancestor	0.15018	0.81658	-0.6623	0.7716366
OR	Or98a2	0.18749	0.17369	-0.024	0.7716366
OR	Or98a6	0.24649	0.30314	-0.044	0.6592839
OR	Or98a2 and 6 ancestor	0.24491	0.30931	-0.33	0.0934421
OR	Or98a4	0.2739	0.14173	**0.0063**	**0.000676304**
OR	Or98a5	0.22865	**1.23866**	**0.01**	0.05279388
OR	Or98a4 and 5 ancestor	0.237	4.11669	-0.4823	**0.01935304**
OR	Or98b1	0.28857	**0.13007**	-0.8492	0.7613693
OR	Or98bLike	0.18605	0.20625	-0.8656	0.5728869
OR	OrN1	0.19137	0.15525	-0.3194	0.1960608
OR	OrN2 copy 1	0.02988	0.07861	-0.0006	0.1278416
OR	OrN2 copy 4	0.14809	0.21155	**0.0008**	0.05293525
OR	OrN2 copy 5	0.2495	0.94941	-0.6183	0.08611496
OR	OrN2 copy 6	0.24826	1.05198	-0.8924	0.1151226
OR	OrN2 copy 1 and 4 ancestor	0.26274	0.16626	-0.4861	0.5728869
OR	Orco	0.26137	0.17749	-0.2037	**0.02049901**

OR67b	*D. grimshawi*	0.24934	0.29184	-0.3355	0.7873258
OR67b	*S. flava* copy 3	0.1041	**1.803**	**0.0375**	**1.44394E-21**
OR67b	*S. flava* copy 2	0.10935	**0.7393**	-0.0208	**1.05769E-10**
OR67b	*S. flava* copy 1	0.11251	**0.62856**	-0.022	**1.5606E-06**
OR67b	*S. pallida*	0.1236	0.0506	-0.3076	**0.01604471**
OR67b	*D. mojavensis*	0.1137	**0.2053**	-0.8484	**0.009320281**
OR67b	*D. virilis*	0.119	0.1185	-1.4528	0.9933245
OR67b	*D. melanogaster*	0.11971	0.04714	-0.0423	0.4999046
OR67b	*D. sechellia*	0.1193	0.0796	-0.0368	0.6982622
OR67b	*D. simulans*	0.1202	0.0197	-0.0523	**0.04609565**
OR67b	*D. yakuba*	0.1198	0.0914	-0.1247	0.614736
OR67b	*D. erecta*	0.1193	0.1051	-0.1126	0.7873258
OR67b	*D. ananassae*	0.1329	0.0303	-1.7359	**5.2654E-10**
OR67b	*D. persimilis*	0.1188	0.1803	-0.0103	0.7873258
OR67b	*D. pseudoobscura*	0.119	0.1149	-0.0078	0.9933245
OR67b	*D. willistoni*	0.1288	0.0427	-1.4866	**1.97605E-05**
OR67b	Subgenus *Drosophila* Ancestor	0.1236	0.0564	-0.9778	**0.01967709**
OR67b	*Sophophora* minus D. *willistoni*	0.1212	0.0711	-0.5393	0.3034497
OR67b	virilis-repleta radiation	0.1196	0.0905	-0.1587	0.7873258
OR67b	Hawaiian radiation ancestor	0.1198	0.0979	-0.2595	0.7817405
OR67b	*Scaptomyza* genus ancestor	0.1221	0.0435	-0.2512	**0.04498955**
OR67b	*S. flava* copy 1, 2 and 3 ancestor	0.1094	**0.4081**	-0.1282	**4.06804E-07**
OR67b	*S. flava* copy 1 and 2 ancestor	0.1135	∞	**0.0276**	**4.5389E-09**
OR67b	*D. simulans* and *D. sechelia* ancestor	0.1205	0.0001	-0.0564	**0.01202915**
OR67b	*D. yakuba* and *D. erecta* ancestor	0.1221	0.0196	-0.1444	**0.00128517**
OR67b	melanogaster subgroup minus Dmel	0.1201	0.048	-0.0727	0.2412147
OR67b	melanogaster subgroup ancestor	0.125	0.0446	-0.5921	**0.003348616**
OR67b	melanogaster group ancestor	0.1207	0.0634	-0.2523	0.4817083
OR67b	pseudoobscura subgroup ancestor	0.1291	0.0342	-0.9693	**2.39766E-06**

Table S1: Parameters for background *versus* foreground branch tests in PAML. * OR = Branch tests for differences in dN/dS rates among *Scaptomyza flava* copies of odorant receptor genes. OR67b = Branch tests for differences in dN/dS rates among all individual branches in a phylogeny of *Or67b* homologs in *Scaptomyza* and *Drosophila* spp. † Terminal branches are indicated with gene names. Ancestral branches are indicated with the term “ancestor” and a list of the terminal branches or the clade subtended.

TableS2 PCR Primers

Primer Name	Sequence	Primer role
67b12Fb	cATGAAGGACTTATTGGATCTGGAGCTAG	CDS amplification
67b1Rb	agcgcaTTATTTGTCTCTCATATTGCTC	CDS amplification
67b2Rb	agcgcaTTATTCATCTCTCATGTTACGC	CDS amplification
67b3Fb	cATGAACTTATTGGATATGGAGCTAG	CDS amplification
67b3Rb	agcgcaTTATTTGTTAGATAAATTACGC	CDS amplification
Sp67bFb	cATGAAAAACCTATTGGACCGGAAG	CDS amplification
Sp67bRb	aaagtacaTCATTTGTTATTCATATTACGCAAAAG	CDS amplification
b1EcoRIF	GACgaattcATGAAGGACTTATTGG	RE cut site addition
b1KpnIR	GACggtaccTTATTTGTCTCTCATATTG	RE cut site addition
b2KpnIR	GACggtaccTTATTCATCTCTCATG	RE cut site addition
b3KpnIR	GACggtaccTTATTTGTTAGATAAATTACG	RE cut site addition
PalEcoRIF	GACgaattcATGAAAAACCTATTGGACC	RE cut site addition
PalKpnIR	GACggtaccTCATTTGTTATTCATATTACG	RE cut site addition

Tables S2: Nucleotides in lower case are either in untranslated sequence (CDS amplification) or are restriction enzyme cut sites (RE cut site addition). CDS amplification primers were used to amplify full *Or67b* CDS sequence from cDNA. Primers labeled “RE cut site addition” were used to engineer restriction enzyme cut-sites via PCR mutagenesis in order to ligate *Or67b* CDS sequences into the pUASTattB plasmid. All sequences are listed in a 5’ to 3’ orientation.

Table S3: Net number of spikes/second; average ± SE

	Empty neuron		Canton-S	
Odors	**spikes #**	**n**	**spikes #**	**n**
ethyl hexanoate	0	7	118±7.7	7
mineral oil	0	7	6.33±1.7	6
acetophenone	0	6	NA	NA
butyl ITC	0	6	NA	NA
mandelonitrile	0	6	NA	NA
cis-3-hexenyl butyrate	0	6	NA	NA
trans-2-pentenal	0	6	NA	NA
geranyl acetate	0	6	NA	NA
mineral oil	0	7	NA	NA

	Dmel67b		Spal67b		Sfla67b1		Sfla67b2		Sfla67b3	
Odors	**spikes #**	**n**	**spikes #**	**n**	**spikes #**	**n**	**spikes #**	**n**	**spikes #**	**n**
apple cider vinegar	96.3±8.0	6	62±10.4	7	-4.33±2.0	6	6.67±4.6	6	15±2.1	6
arugula	19.7±3.0	6	14±3.4	7	64±7.8	6	24±8.7	6	22.3±2.3	6
wasabi	2.67±2.0	6	2.67±1.11	6	15.3±1.9	8	16.2±2.5	8	13.7±4.4	6
horseradish	3.67±1.8	6	-0.33±1.0	6	8.75±1.3	8	12.9±2.0	8	31.7±4.4	6
turnip	1±1.8	6	0.67±0.7	6	11.8±1.6	8	22±2.7	8	34.3±1.4	6
daikon	2±3.2	6	-0.67±0.8	6	14±2.4	8	17.1±3.4	8	19±3.4	6
beet	8±3.8	6	-0.33±1.1	6	2±1.30	6	-0.33±1.7	6	4.33±2.2	6
Dmel67b activators										
acetophenone	176±18	7	78±2.4	20	3.27±1.2	11	4.5±2.0	8	1.57±1.3	14
cis-3-hexen-1-ol	56.9±20	7	22±4.1	7	8.67±2.0	6	6.75±1.3	8	2.67±2.3	6
4-methylcyclohexenol	80.7±8.7	6	33±4.4	13	8.89±4.3	9	1.56±1.4	9	2.67±1.2	6
phenethyl alcohol	140±19	8	26.3±4.5	6	2.67±1.2	6	1±1.2	6	3.67±1.5	6
1-hexanol	118±13	7	19.14286	7	13.7±3.8	6	10.4±4.6	9	8±1.9	6
ethyl (S)-(+)-3-hydroxybutanoate	15.7±3.3	7	12±2.8	7	4.33±4.4	6	10.4±2.9	9	8±2	6
2-hexanol	12.3±5.2	8	11.7±2.8	7	7.33±2.1	6	9.5±1.8	8	7±3.1	6
benzyl alcohol	48.6±2.9	6	14.3±3.7	7	-1.33±0.8	6	6.75±1.8	8	5.67±1.4	6
2-hexanone	40±16	7	7.14±2.0	7	9.33±4.8	6	7.5±2.0	8	7.33±3.5	6
hexyl-formate	39.3±8.7	6	16.3±5.6	7	7±2.0	6	8.89±4.5	9	3±0.9	6
phenethyl aldehyde	51.4±10	7	29.4±3.8	7	2±2.3	6	2.86±3.0	7	1±0.7	6
2-heptanone	28±4.1	7	13.1±2.3	7	6.33±2.4	6	15.3±2.5	9	6±1.9	7
ITCs										
butyl ITC	4.57±1.6	7	15±4.2	6	196±15	7	22.7±2.8	6	171±11	7
ethyl ITC	0.33±1.5	6	2.33±0.95	6	24±2.7	6	3.33±3.9	6	13±1.7	6
isobutyl ITC	1.67±2.4	6	5.33±2.6	6	74±12	7	4.33±1.8	6	139±17	7
sec-butyl ITC	4.29±1.0	7	5±1.8	6	9.14±2.7	7	5.33±2.3	6	121±17	8
allyl ITC	3.43±0.8	7	9.75±4.2	8	28.9±5.3	7	6±2.4	7	4.75±3.7	8
3-methylthio propyl ITC	2±1.8	6	6.33±2.2	6	179±9.2	6	33±6.0	6	137±17	8
benzyl ITC	2.29±1.4	7	3.75±1.9	8	81.7±14.4	7	3.14±1.3	7	134±14	8
phenethyl ITC	6.57±2.2	7	5.25±2.8	8	4.8±1.3	10	1.14±0.86	7	158±15	8
3-methoxybenzyl ITC	-0.67±1.1	6	7±3.3	6	4.57±2.2	7	1.67±0.80	6	3.14±2.1	7
Nitriles										
mandelonitrile	45.3±11	6	1±1	6	1.33±1.8	6	-0.29±0.7	7	4±3.0	6
adiponitrile	2.67±2.5	6	0.33±0.33	6	0.33±0.3	6	0.67±2.2	6	4.33±1.8	6
propionitrile	5.33±1.6	6	1.33±0.4	6	2.3±2.0	6	1.33±1.1	6	4.33±2.5	6
GLVs										
cis-3-hexenyl butyrate	91±21	7	49.3±8.0	6	5±2.6	8	2±1.8	6	11.8±2.5	8
trans-2-hexen-1-ol	33±6.0	6	51±11	6	23.5±5.6	8	3±2.5	6	6.29±2.2	7
trans-2-hexenyl acetate	55.7±19	7	34±6.8	6	2±2.1	6	17.3±2.5	6	10.3±1.9	8
trans-2-hexenyl butyrate	29.7±6.7	6	35.6±8.2	6	1.71±1.0	7	4±1.5	6	12±4.3	7
cis-3-hexenyl acetate	43.3±9.3	6	13.7±2.6	6	1.67±1.7	6	16±5.3	8	11±5.8	6
TrpA1 activators/										

electrophiles										
trans-2-pentenal	27.1±20	7	6.33±0.8	6	4.33±2.9	6	4±1.4	6	4±1.3	6
citronellal	1.43±1.6	7	7±2.3	6	4.57±1.6	7	9.14±3.5	7	12±2.8	11
cinnamaldehyde	12.3±2.8	7	9±3.8	6	9.25±2.7	8	3±1	6	6±1.7	12
acrorelin	2.67±2.6	6	6.33±2.2	6	6.67±1.9	6	7±4.3	6	3.33±1.3	6
iodoacetamide	1.43±1.4	7	6±1.9	6	7.33±1.6	6	6±2.4	6	4±1.7	6
formaldehyde	3.14±2.0	7	5.33±1.8	6	6±2.9	6	3±1.4	6	2±1.0	6
N-methylmaleimide	3.71±1.0	7	8.67±2.6	6	7.33±1.8	6	10±1.9	6	3±1.3	6
N-hydroxysuccinimide	1.71±1.3	7	4.67±2.5	6	4.67±2.6	6	8.67±2.3	6	2±0.7	6
methyl salicylate	-3±1.8	7	0±0.5	6	3±3	6	-0.57±1.8	7	5.33±4.2	6
S-allyl 2-propene-1-sulfinothioate	5.66±1.0	7	-0.33±0.8	6	3.67±1.5	6	0.57±1.1	7	3±1.5	6
diallyl disulfide	3.33±3.3	7	0.67±0.8	6	1.33±0.7	6	1.14±0.6	7	3.67±2.1	6
Others										
geranyl acetate	5.67±1.0	6	26±6.5	6	8.5±2.4	8	4.67±2.0	6	5.25±1.4	8
limonene	2.29±2.4	7	5±4.1	6	4.33±1.6	6	1±0.7	6	2.71±1.5	14
indol-3-carbinol	4±1.5	6	3.33±2.6	6	5.67±1.6	6	8.67±1.1	6	3.33±0.8	6
benzyl thyocyanate	2.57±1.4	7	7.67±1.4	6	8.67±2.4	6	5±1.3	6	8.67±2.8	6
Solvent control										
DMSO	2.86±1.6	7	10.7±3.2	6	3.33±1.0	6	7.67±1.4	6	4.33±2.9	6
mineral oil	3.73±1.2	15	0.91±0.87	11	1±1.4	6	1±1.8	6	0±0.38	11

	Sfla67b1		Sfla67b3	
odorants	**spikes #**	**n**	**spikes #**	**n**
3-methylthio propyl ITC				
1/100	114±18	8	127±13	6
1/1,000	64±11	8	27.7±7.1	6
1/10,000	27.9±4.6	8	11.7±5.3	6
1/100,000	12±3.3	9	10±4.0	6
butyl ITC				
1/100	147±19	10	161±16	6
1/1,000	46.8±6.6	9	50.7±8.1	6
1/10,000	25.6±7.3	8	19.7±6.2	6
1/100,000	14.25±5	9	7.33±3.4	6
isobutyl ITC				
1/100	40.6±9.0	8	131±14	6
1/1,000	6.3±2.3	8	31.7±5.6	6
1/10,000	5.63±2.7	8	9±3.8	6
1/100,000	8.25±1.8	9	6±5.2	6
sec-butyl ITC				
1/100	5±1.7	9	124±13	6
1/1,000	4.5±1.6	9	26.3±4.2	6
1/10,000	5.63±1.8	8	13.7±4.6	6
1/100,000	10.5±3.5	8	9±4.5	6
benzyl ITC				
1/100	94.5±14.1	10	123±13	6
1/1,000	16.5±5.1	9	27.7±9.4	6
1/10,000	8.625±3.6	8	8±1.4	6
1/100,000	10.5±3.2	9	13±5.0	6
phenethyl ITC				
1/100	5.25±2.8	9	147±17	6
1/1,000	8.5±3.0	8	74±18	6
1/10,000	8.71±4.1	7	26.3±7.4	6
1/100,000	8±2.9	7	9.33±5.2	6
mineral oil	1±1.4	6	0±0.4	11

Tables S3: Responses (net number of spikes/second; average ± SE) of the ab3 sensilla of flies expressing either no ORs (Empty neuron), wild-type *Or22a* (Canton-S), *Dmel Or67b, Spal Or67b, Sfla Or67b1, Sfla Or67b2 or Or67b3* to stimulation with the odors and number of recordings are denoted.

Figure 1

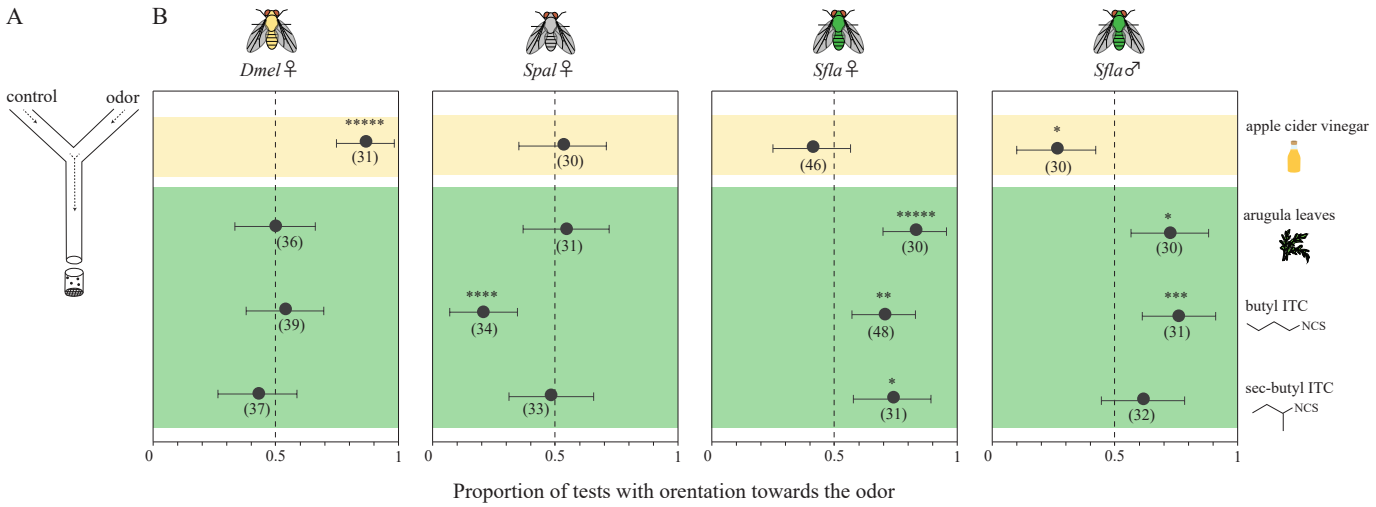
A
B
control
odor
Dmel ♀
Spal ♀
Sfla ♀
Sfla ♂
*****
(31)
(36)
(39)
(37)
(30)
(31)
****
(34)
(33)
(46)
*****
(30)
**
(48)
*
(31)
*
(30)
*
(30)
***
(31)
(32)
apple cider vinegar
arugula leaves
butyl ITC
NCS
sec-butyl ITC
NCS
0
0.5
1
Proportion of tests with orentation towards the odor

Figure 2

A

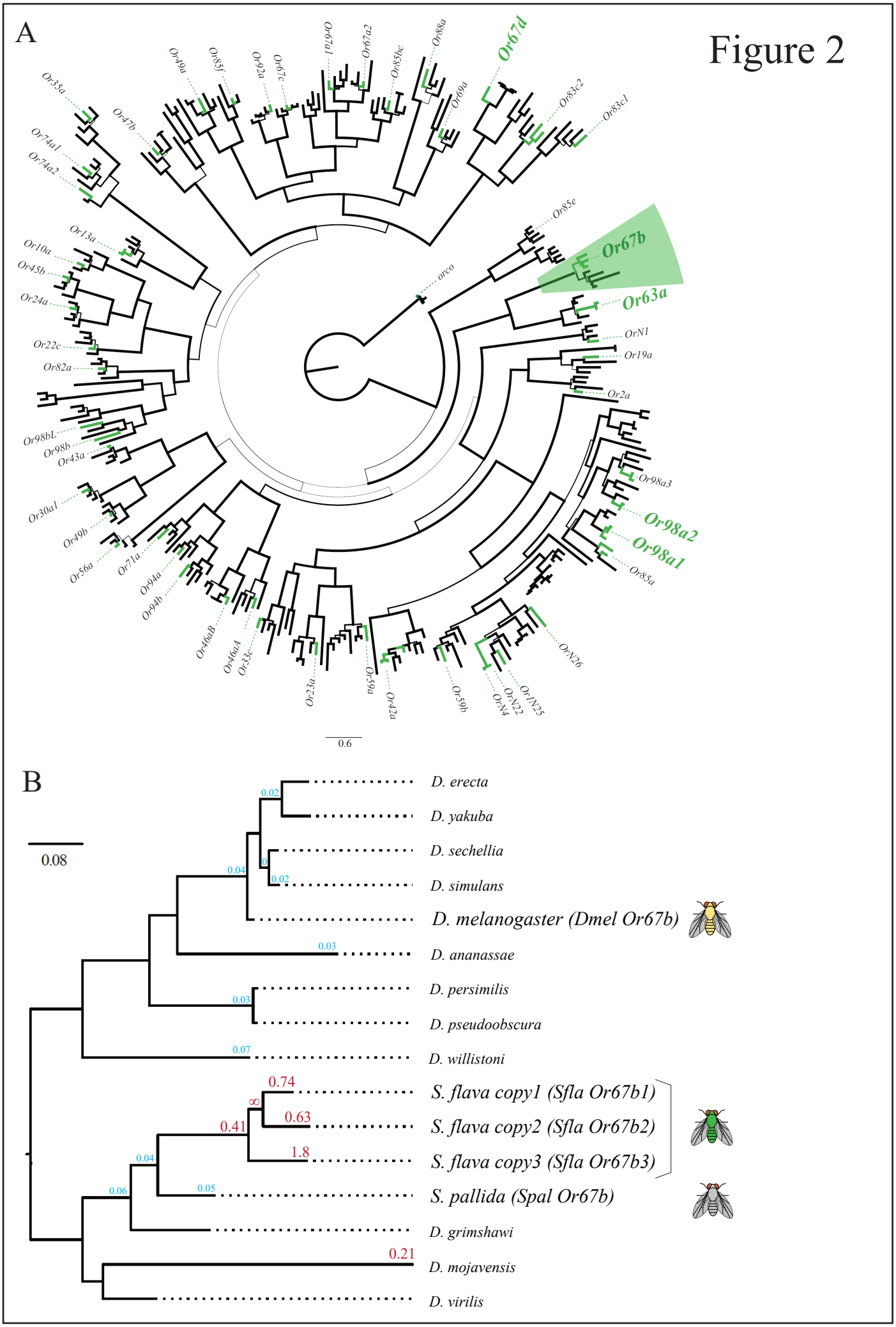
Or67d
Or67b
Or63a
Or98a2
Or98a1
Or35a
Or47b
Or74a1
Or74a2
Or49a
Or85f
Or92a
Or67c
Or67d1
Or67a2
Or85bc
Or88a
Or69a
Or83c2
Or83c1
Or85e
Or13a
Or10a
Or45b
Or24a
Or22c
Or82a
Or98bL
Or98b
Or43a
Or30a1
Or49b
Or56a
Or71a
Or94a
Or94b
Or46aB
Or46aA
Or33c
Or23a
Or59a
Or42a
Or59b
OrN4
OrN22
OrN25
OrN26
Or85a
Or98a3
Or2a
Or19a
OrN1
orco
0.6

B

0.08
D. erecta
D. yakuba
D. sechellia
D. simulans
D. melanogaster (Dmel Or67b)
D. ananassae
D. persimilis
D. pseudoobscura
D. willistoni
S. flava copy1 (Sfla Or67b1)
S. flava copy2 (Sfla Or67b2)
S. flava copy3 (Sfla Or67b3)
S. pallida (Spal Or67b)
D. grimshawi
D. mojavensis
D. virilis
0.02
0.04
0
0.02
0.03
0.03
0.07
0.74
∞
0.63
0.41
1.8
0.04
0.06
0.05
0.21

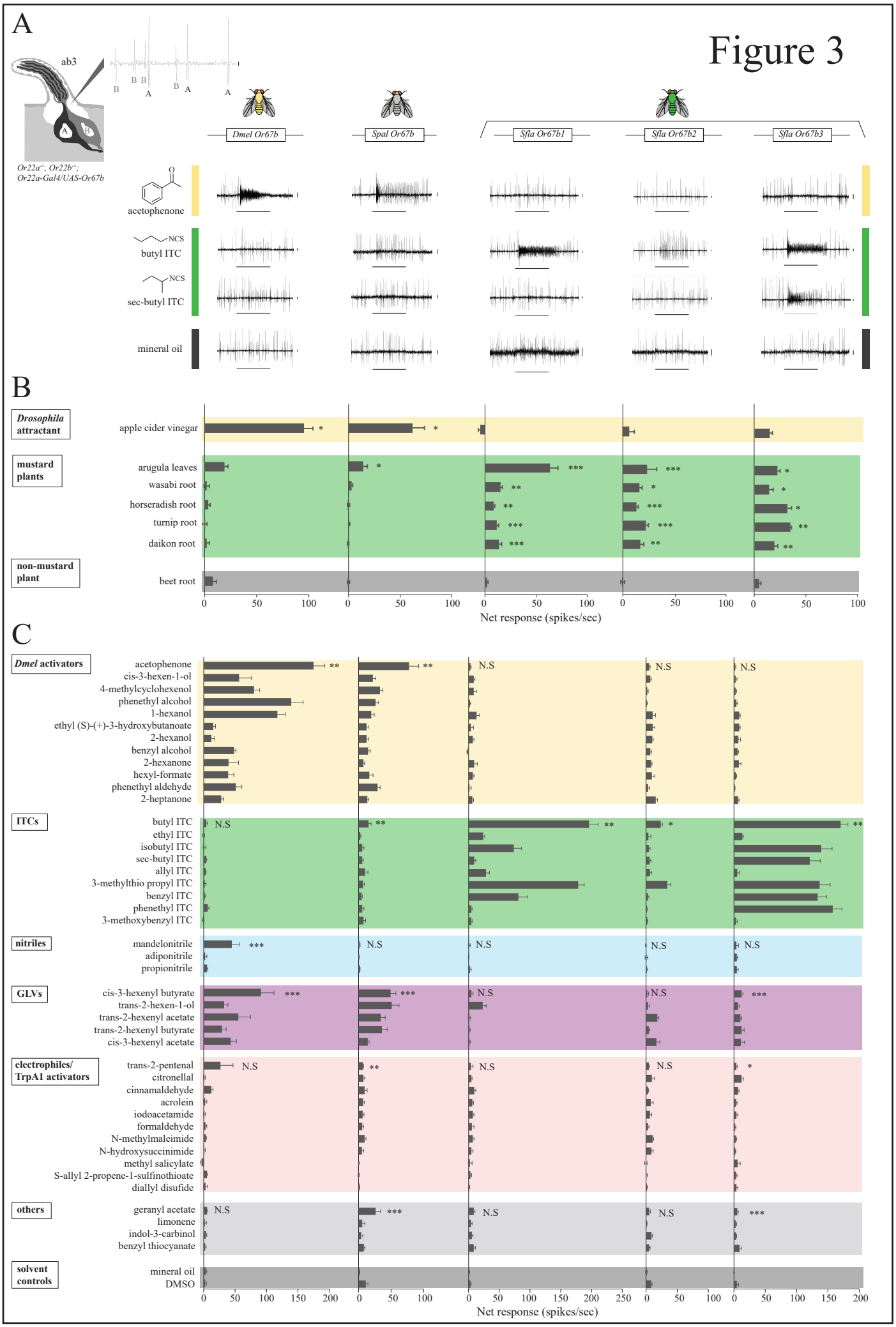
Figure 3
A
ab3
B
B B
A
B A
A
Or22a-/-, Or22b-/-;
Or22a-Gal4/UAS-Or67b
Dmel Or67b
Spal Or67b
Sfla Or67b1
Sfla Or67b2
Sfla Or67b3
acetophenone
butyl ITC
sec-butyl ITC
mineral oil
NCS
B
Drosophila attractant
apple cider vinegar
mustard plants
arugula leaves
wasabi root
horseradish root
turnip root
daikon root
non-mustard plant
beet root
Net response (spikes/sec)
C
Dmel activators
acetophenone
cis-3-hexen-1-ol
4-methylcyclohexenol
phenethyl alcohol
1-hexanol
ethyl (S)-(+)-3-hydroxybutanoate
2-hexanol
benzyl alcohol
2-hexanone
hexyl-formate
phenethyl aldehyde
2-heptanone
ITCs
butyl ITC
ethyl ITC
isobutyl ITC
sec-butyl ITC
allyl ITC
3-methylthio propyl ITC
benzyl ITC
phenethyl ITC
3-methoxybenzyl ITC
nitriles
mandelonitrile
adiponitrile
propionitrile
GLVs
cis-3-hexenyl butyrate
trans-2-hexen-1-ol
trans-2-hexenyl acetate
trans-2-hexenyl butyrate
cis-3-hexenyl acetate
electrophiles/ TrpA1 activators
trans-2-pentenal
citronellal
cinnamaldehyde
acrolein
iodoacetamide
formaldehyde
N-methylmaleimide
N-hydroxysuccinimide
methyl salicylate
S-allyl 2-propene-1-sulfinothioate
diallyl disufide
others
geranyl acetate
limonene
indol-3-carbinol
benzyl thiocyanate
solvent controls
mineral oil
DMSO
N.S
Net response (spikes/sec)

Figure 4

A

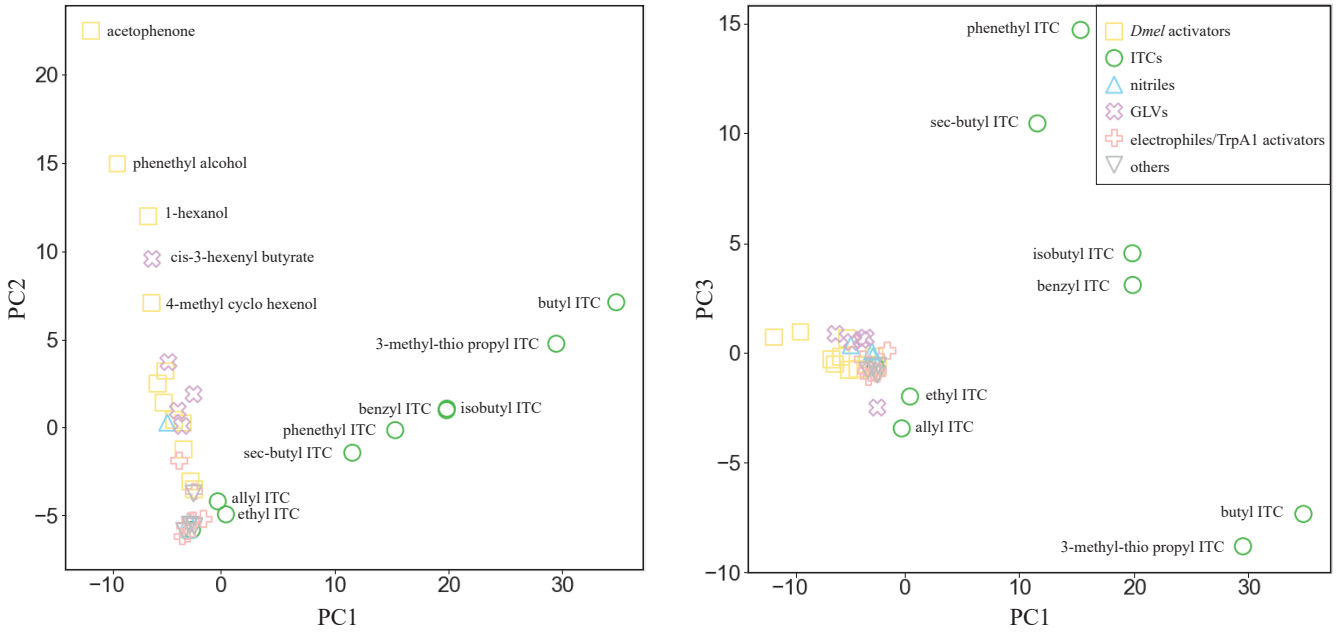
acetophenone
phenethyl alcohol
1-hexanol
cis-3-hexenyl butyrate
4-methyl cyclo hexenol
butyl ITC
3-methyl-thio propyl ITC
benzyl ITC
isobutyl ITC
phenethyl ITC
sec-butyl ITC
allyl ITC
ethyl ITC
PC1
PC2
PC3
Dmel activators
ITCs
nitriles
GLVs
electrophiles/TrpA1 activators
others

B

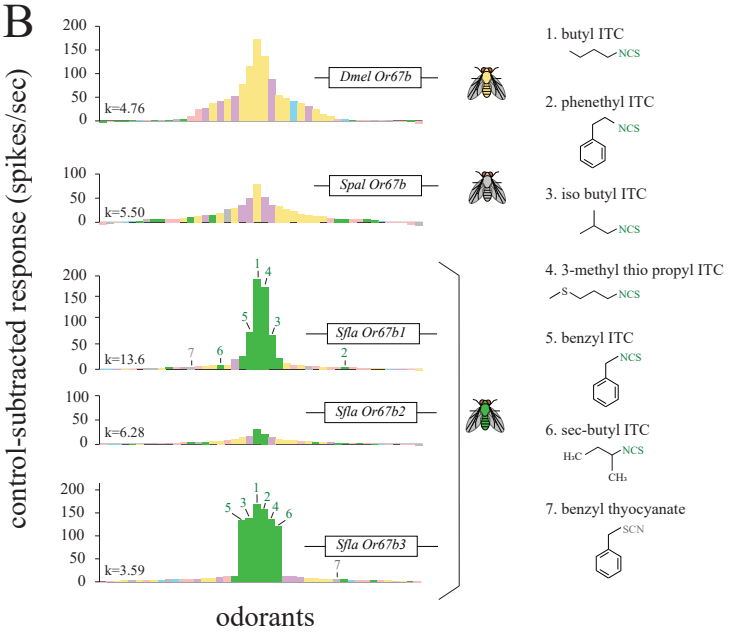
control-subtracted response (spikes/sec)
Dmel Or67b
k=4.76
Spal Or67b
k=5.50
Sfla Or67b1
k=13.6
Sfla Or67b2
k=6.28
Sfla Or67b3
k=3.59
odorants
1. butyl ITC
2. phenethyl ITC
3. iso butyl ITC
4. 3-methyl thio propyl ITC
5. benzyl ITC
6. sec-butyl ITC
7. benzyl thyocyanate

C

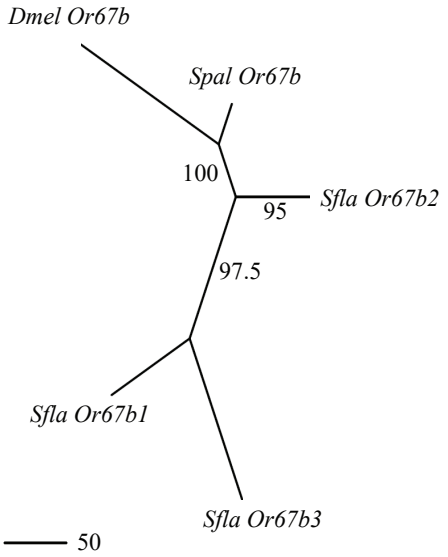
Dmel Or67b
Spal Or67b
Sfla Or67b2
Sfla Or67b1
Sfla Or67b3
100
95
97.5
50

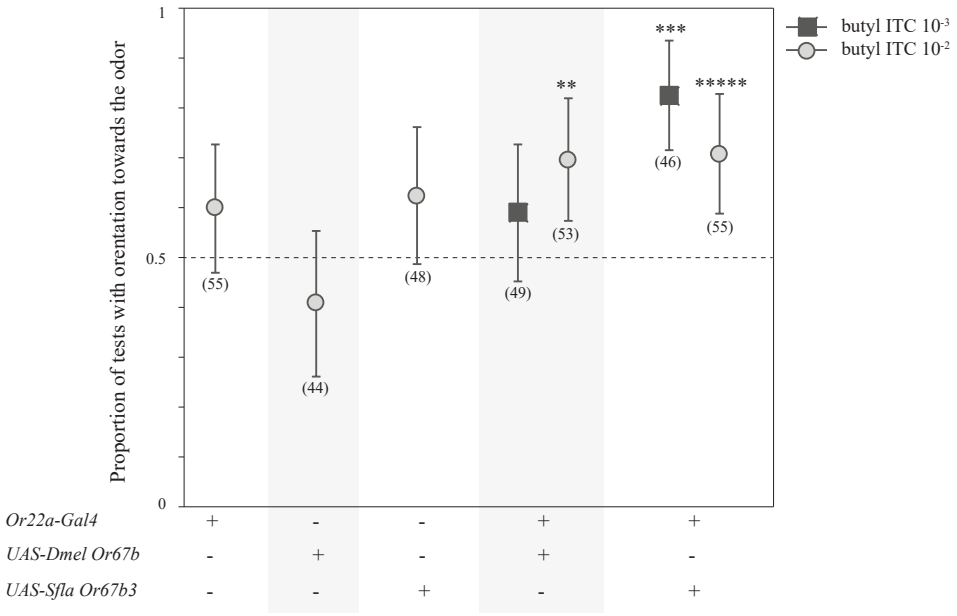
Proportion of tests with orientation towards the odor
1
0.5
0
butyl ITC 10-3
butyl ITC 10-2
***
**
*****
(55)
(44)
(48)
(49)
(53)
(46)
(55)
Or22a-Gal4 + - - + +
UAS-Dmel Or67b - + - + -
UAS-Sfla Or67b3 - - + - +

Figure 5

Figure 6

A

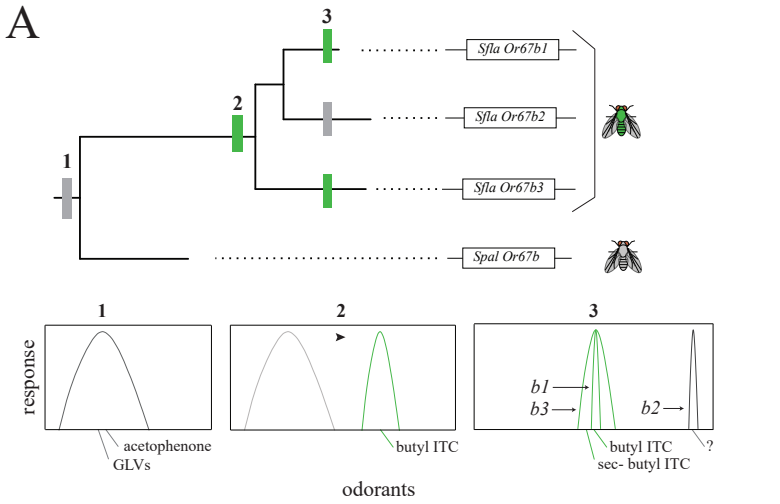
1
2
3
Sfla Or67b1
Sfla Or67b2
Sfla Or67b3
Spal Or67b
response
acetophenone
GLVs
butyl ITC
b1
b3
b2
butyl ITC
sec- butyl ITC
?
odorants

B

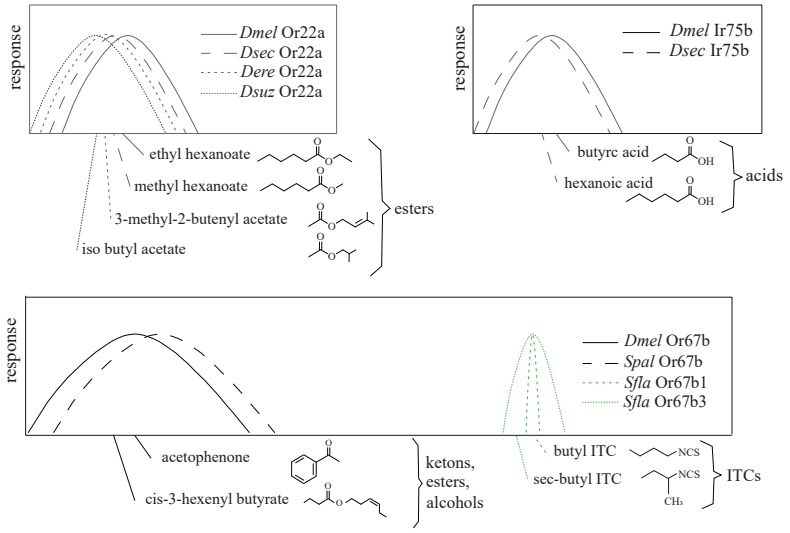
response
Dmel Or22a
Dsec Or22a
Dere Or22a
Dsuz Or22a
ethyl hexanoate
methyl hexanoate
3-methyl-2-butenyl acetate
iso butyl acetate
esters
Dmel Ir75b
Dsec Ir75b
butyrc acid
hexanoic acid
acids
Dmel Or67b
Spal Or67b
Sfla Or67b1
Sfla Or67b3
acetophenone
cis-3-hexenyl butyrate
ketons,
esters,
alcohols
butyl ITC
sec-butyl ITC
ITCs

Figure S1

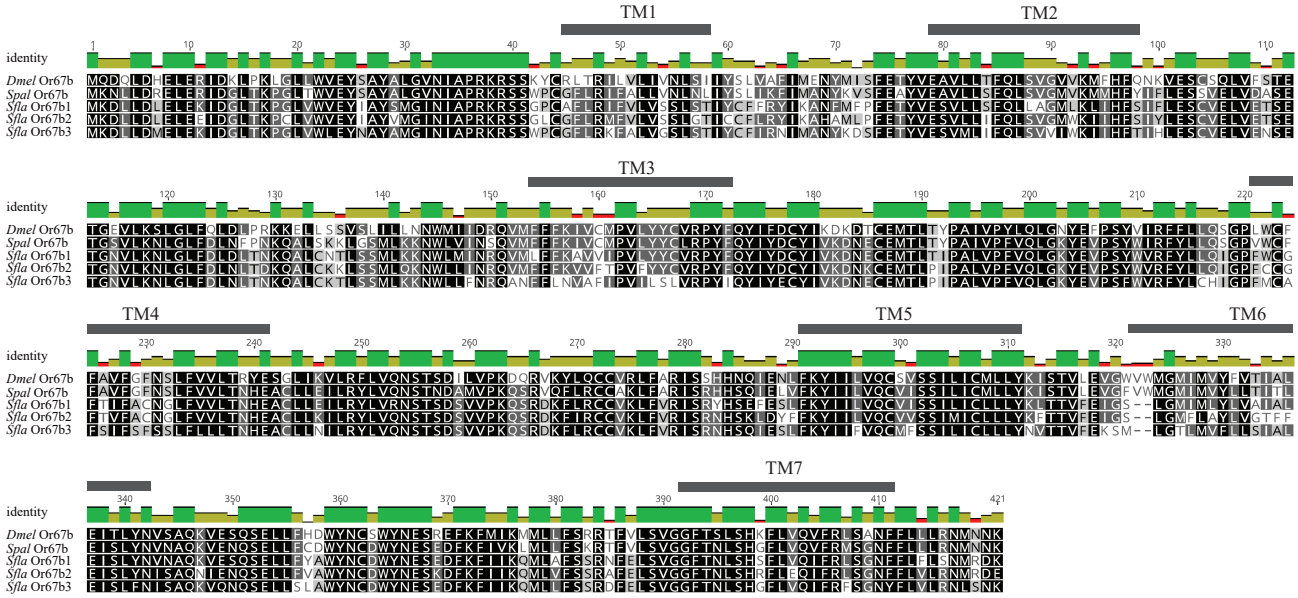
TM1
TM2
TM3
TM4
TM5
TM6
TM7
identity
Dmel Or67b
Spal Or67b
Sfla Or67b1
Sfla Or67b2
Sfla Or67b3

Figure S2

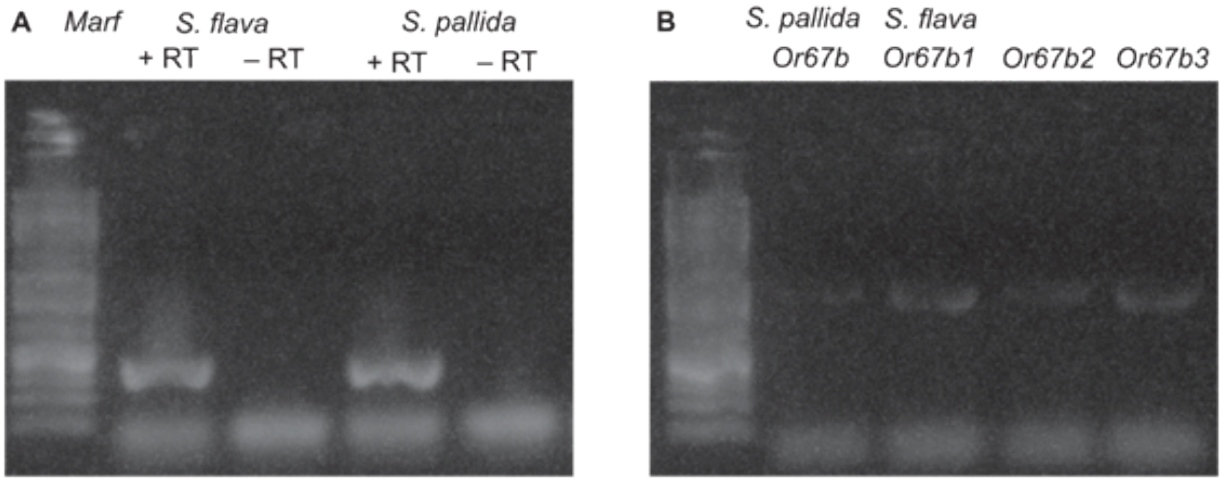
A
Marf
S. flava
+ RT
– RT
S. pallida
+ RT
– RT
B
S. pallida
Or67b
S. flava
Or67b1
Or67b2
Or67b3

Figure S3

A

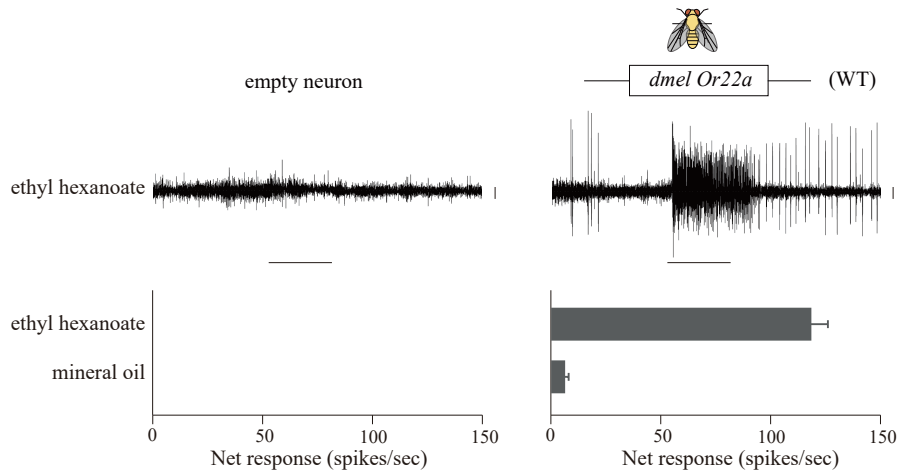

B

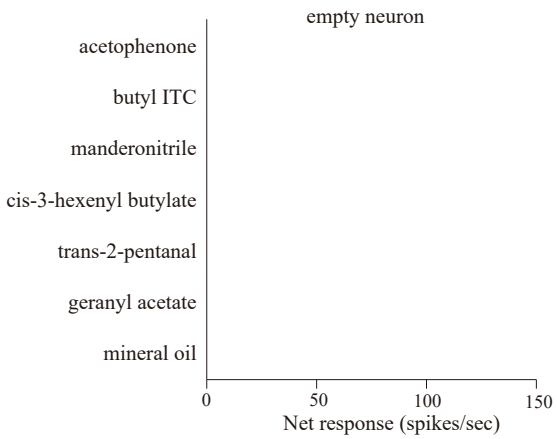

C

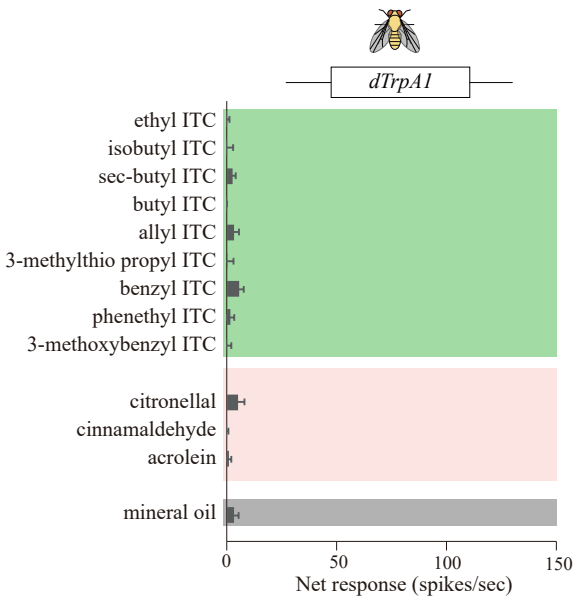

Figure S4

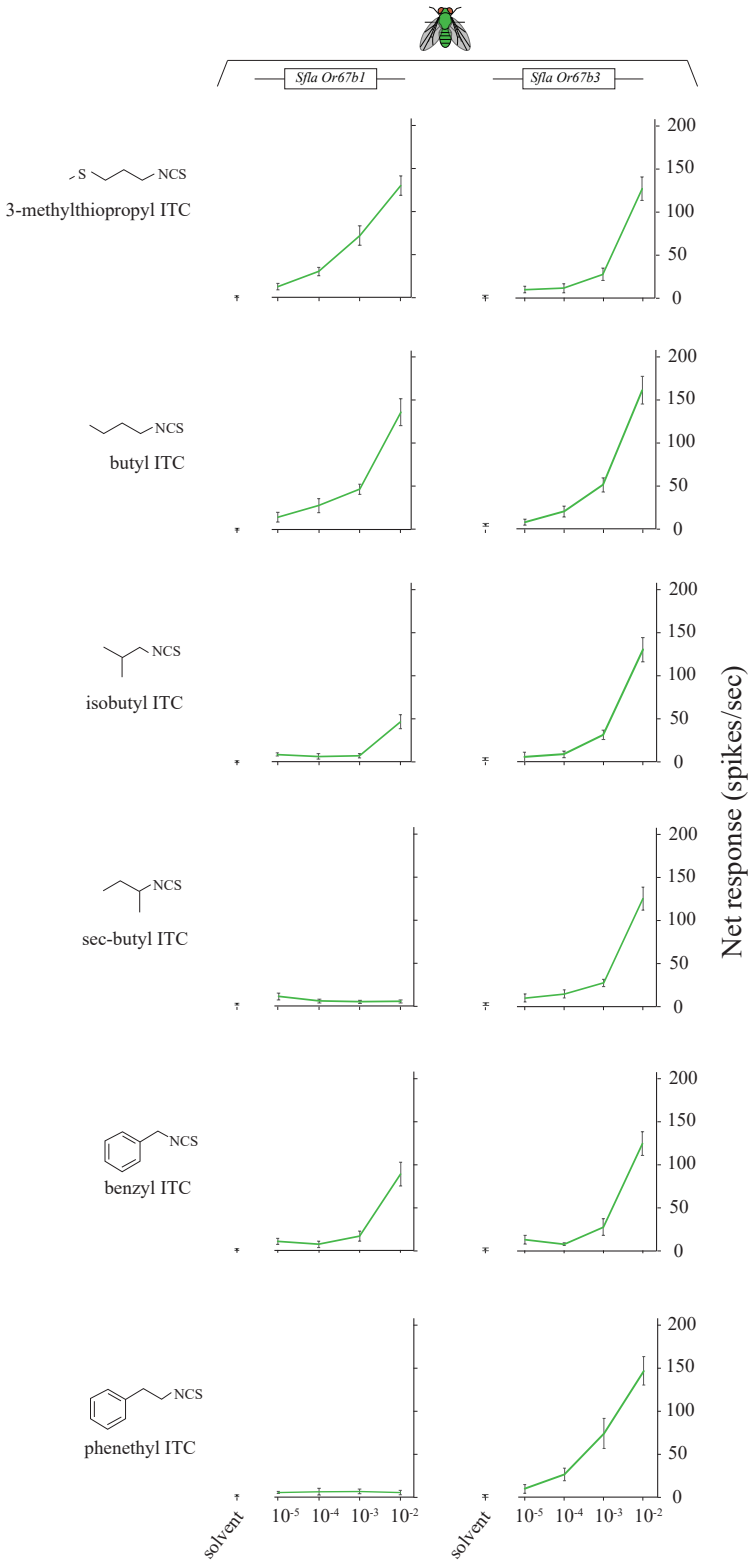
Sfla Or67b1
Sfla Or67b3
3-methylthiopropyl ITC
butyl ITC
isobutyl ITC
sec-butyl ITC
benzyl ITC
phenethyl ITC
NCS
S
Net response (spikes/sec)
200
150
100
50
0
solvent
10-5
10-4
10-3
10-2
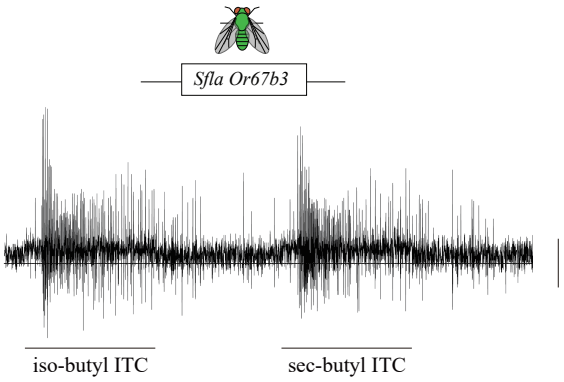
Figure S5